Naval Surface Warfare Center
Carderock Division
West Bethesda, MD 20817-5700

NSWCCD-61-TR–2006/07 April 2006

Survivability, Structures, and Materials Department
Technical Report

Mechanism of Corrosion Product Growth on Nickel Aluminum Bronze/Ammonia or Seawater Interface: Modeling Based on Chemical Reaction Kinetics

by

A. Srinivasa Rao

NSWCCD-61-TR–2006/07 Mechanism of Corrosion Product Growth on Nickel Aluminum Bronze/Ammonia or Seawater Interface: Modeling Based on Chemical Reaction Kinetics

Naval Surface Warfare Center
Carderock Division
West Bethesda, MD 20817-5700

NSWCCD-61-TR–2006/07 April 2006

Survivability, Structures, and Materials Department
Technical Report

Mechanism of Corrosion Product Growth on Nickel Aluminum Bronze/Ammonia or Seawater Interface: Modeling Based on Chemical Reaction Kinetics

by

A. Srinivasa Rao

This page intentionally left blank

REPORT DOCUMENTATION PAGE

Form Approved
OMB No. 0704-0188

1. REPORT DATE *(DD-MM-YYYY)*	**2. REPORT TYPE**	**3. DATES COVERED** *(From - To)*
04-2006	Research and Development	

4. TITLE AND SUBTITLE

Mechanism of Corrosion Product Growth on Nickel Aluminum Bronze /Ammonia or Seawater Interface: Modeling Based on Chemical Reaction Kinetics

5a. CONTRACT NUMBER

5b. GRANT NUMBER

5c. PROGRAM ELEMENT NUMBER
060247N

6. AUTHOR(S)

A. Srinivasa Rao

5d. PROJECT NUMBER

5e. TASK NUMBER

5f. WORK UNIT NUMBER

7. PERFORMING ORGANIZATION NAME(S) AND ADDRESS(ES) AND ADDRESS(ES)
NAVAL SURFACE WARFARE CENTER
CARDEROCK DIVISION (
CODE 612, METALS ENGINEERING BRANCH)
9500 MACARTHUR BLVD
WEST BETHESDA MD 20817-5700

8. PERFORMING ORGANIZATION REPORT NUMBER

NSWCCD-61-TR-2007/06

9. SPONSORING / MONITORING AGENCY NAME(S) AND ADDRESS(ES)

10. SPONSOR/MONITOR'S ACRONYM(S)

11. SPONSOR/MONITOR'S REPORT NUMBER(S)

12. DISTRIBUTION / AVAILABILITY STATEMENT
Distribution unlimited. Approved for public release.

13. SUPPLEMENTARY NOTES

14. ABSTRACT

The open circuit potentials (versus SCE) were measured for nickel aluminum bronze (NAB) samples after exposure to seawater and 90%-10%, 80%-20% and 50%-50% water ammonia solutions for up to 34 days, in order to model the electrochemical reaction. The results suggest that the normalized open circuit potentials (versus SCE), can be used to determine the reaction kinetics. The results also suggest that the data (normalized potentials) obtained for up to 10 days shows significant scatter and this scatter is probably due to selective corrosion of different metals and /or the induction period for the corrosion process. The data obtained after 10 days shows a specific trend. The over all reaction for the corrosion of NAB in 90%-10% and 80%-20% water - ammonia solution is primarily diffusion controlled process. The order of reaction during the fast oxide growth suggests that only the concentration of the metal is changing with time. The overall reaction for NAB in 50%-50% water ammonia solution is controlled both by the diffusion process and also a change in concentration of metal. In order to compare the data obtained from open circuit potentials with the data obtained from structural analysis during the corrosion process, the electrochemical kinetics parameters were determined from earlier data on the change in the structure of nickel , nickel - copper alloy due to cathodic and anodic electrochemical reaction in KOH and seawater for reaction up to 24 hours. The results suggest that the kinetic processes are dominated by selective chemical reactivity of copper and nickel.

15. SUBJECT TERMS
Nickel Aluminum Bronze; Ammonia; Seawater; Reaction Kinetics

16. SECURITY CLASSIFICATION OF:			**17. LIMITATION OF ABSTRACT**	**18. NUMBER OF PAGES**	**19a. NAME OF RESPONSIBLE PERSON**
a. REPORT	**b. ABSTRACT**	**c. THIS PAGE**			Dr. A. Srinivasa Rao
UNCLASSIFIED	**UNCLASSIFIED**	**UNCLASSIFIED**	**SAR**	62	**19b. TELEPHONE NUMBER** *(include area code)* 301-227-5141

This page intentionally left blank

Contents

Figures

Figures (Cont)

Figures (Cont)

Tables

Administrative Information

The work described in this report was performed at the Naval Surface Warfare Center, Carderock Division (NSWCCD), West Bethesda, MD, in the Survivability, Structures and Materials Department (Code 60) by personnel from the Metals Division (Code 61). The project was funded from the Code 61 Internal Overhead Funds.

Acknowledgements

The author would like to thank Drs. C. Wong (Code 612) and K. L. Vasanth (Code 613) for providing experimental data on the open circuit potentials measured for nickel aluminum bronze samples in ammonia or seawater solution. The author would also like to thank Prof. C. Gilmore and Mr. Paul Goldey, of the Institute of Materials Science, The George Washington University, for permitting the author to conduct experiments in the thin film laboratory. The author also acknowledges the use of the University x-ray diffraction facilities purchased by the Geology Department of the George Washington University under an NSF grant to Prof. Fred Siegel

Executive Summary

This investigation was undertaken to model the measured open circuit potentials (versus SCE) obtained for nickel aluminum bronze (NAB) samples after exposure to seawater and 90%-10%, 80%-20% and 50%-50% water ammonia solutions for up to 34 days in terms of electrochemical reaction. The results suggest that the normalized open circuit potentials (versus SCE) can be used to determine the reaction kinetics. The results also suggest that the data (normalized potentials) obtained for up to 10 days shows significant scatter and this scatter is probably due to selective corrosion of different metals and or the induction period for the corrosion process. The data obtained after 10 days shows (with in the limits of the measurement error) specific trend.

The over all reaction for the corrosion of NAB in 90%-10% and 80%-20% water - ammonia solution is primarily diffusion controlled process. The order of reaction during the fast oxide growth (is one) suggests that only the concentration of the metal is changing with time. Therefore, it is reasonable to suggest that the oxide formed during this process is nearly uniform with fine mud cracking. The overall reaction for NAB in 50%-50% water ammonia solution is controlled both by the diffusion process and also a change in concentration of metal. The results conclude that the oxide is formed on the surface at a much faster rate, is not uniform and it suffers from severe mud cracking type surface topology.

In order to compare the data obtained from open circuit potentials with the data obtained from structural analysis during the corrosion process the electrochemical kinetic parameters were determined from the earlier data on the change in the structure of the Ni, Cu-Ni alloy due to cathodic and anodic electrochemical reaction in KOH and seawater for reaction up to 24 hours. The results suggested that the kinetics is dominated by the selective chemical reactivity of copper and nickel.

The present analysis proposes that a new and thorough investigation is needed to establish a direct correlation between the open circuit potential measurement, and the analysis based on structure for NAB samples in seawater and or other reactive agents.

Introduction

Process modeling is an efficient method to understand a specific process and optimize the process variables. Modeling requires first training a sequence of logical realities and then deriving proper conclusions as dependable mathematical relationships. For example, during simple corrosion of a metal, although one observes the formation of an oxide layer on the metal surface, other properties such the potential, structure and mechanical strength also change. Since these properties are related to the chemistry and physics of the metal, it is possible to correlate all the inter-related properties. In order to ascertain some fundamental relationships between the rate of corrosion and the order of the chemical reaction and the nature of the oxide film, an experimental database was obtained from systematic corrosion studies.

The aim of the present study is to collect the available data on the corrosion kinetic study and test whether the developed kinetics process model can predict the growth and morphology of corrosion products. An ongoing program to reduce maintenance requirements and expedite repair of naval nickel aluminum bronze components conducted a systematic study on the growth of corrosion products as a function of reaction time [1]. During that investigation, the open circuit potentials (OCP) for the nickel aluminum bronze samples when exposed to ammonia or seawater were measured continuously for over 33 days. For this study, the OCP data was re-analyzed using a model developed to predict the rate and nature of the corrosion products assuming that the oxide growth on the entire sample surface occurs uniformly, and once the reaction is initiated the oxide grows continuously.

Similarly, the information on the change in the structure of the metal at the metal/corroding solution interface was collected from an earlier program on the electrochemical reaction between nickel, copper-nickel alloy in KOH solution, [2,3]. The change in the structure of the metal was analyzed using the present model.

Experimental Procedure

Materials and Testing

The data used in this study was obtained from other investigations. The first set of data was collected from a corrosion study involving the measurement of open circuit potentials during the electrochemical reaction for 33 days. The second set of results was collected from in-situ examination of the nucleation and growth of oxide film at the solid – liquid interface during an electrochemical reaction.

Similarly, some earlier published information on the change in the structure of surface oxide film in nickel, and copper – nickel alloys in KOH solution over 24 hour period [2,3] was also used in for the present modeling studies.

The chemical kinetics modeling for the corrosion of nickel aluminum bronze in ammonia solution and/or seawater was carried out from some corrosion test data (represented as the change in open circuit potential) in which 16 as-received and heat treated nickel aluminum bronze (NAB) samples were submerged in 10%, 20%, 50% ammonia solution, and simulated seawater. For convenience all the studies in simulated seawater were labeled as in seawater. A total of 12 samples were exposed to ammonia solution and 4 samples were exposed to seawater solution. Using a standard electrochemical test procedure, the open circuit potential of NAB was measured against a standard Ag- calomel electrode for about 33 days [1].

The electrical potential of the samples was measured against a standard calomel electrode (SCE) reference electrode for up to 35 days and the measured potentials (versus SCE) versus the reaction times are given in Tables 1 and 2 respectively.

As-received commercial fine 12.5 μm thick Nickel foils and commercial 90-10, 70-30 copper nickel alloy sheets were thinned to about 12.5 μm thick, were immersed in 5 M KOH. The thin foils were subjected to either cathodic or anodic reaction with the application of a constant negative or positive potential. The change in the structure of the foil surface was

followed using x-ray diffraction. The experimental details were given in our earlier reports [2,3] and the data on the change in the structure was used for this present modeling study.

Theory

In general, it can be hypothesized that as the electrochemical reaction progresses, the reaction products continue to grow (Figure 1). While the change in the metal surface concentration that is actively taken part in the electrochemical process has a finite functionality (i.e. the concentration changes with time), the concentration of the corroding media remains constant (the solution concentration remains unchanged or the change in the concentration ratio between the metal and solution is negligible). Under these conditions, the kinetics of the electrochemical process can be represented as follows [4]:

$$\mathbf{(dw/dt) \propto - \{(dw_{oxide}/dt) \ or} \text{ or}$$

$$\mathbf{(dw/dt) = A \{ (dw_{oxide}/dt)} \quad [1]$$

where A is a constant.

The overall oxide formation depends upon the reaction kinetics and it will be fast at the beginning and very slow at the end. Generally the slow reaction stage is preceded with an intermediate reaction zone. The overall oxide formation during any one of the stages could depend upon several parameters such as direct chemical reaction with the metal surface, a reaction process that involves the diffusion of reacting liquid to reach the new metal surface, a reverse kinetics due to the reduction of formed metal oxide to the metal etc. All the above chemical processes influence the chemical reaction at any given time. Figure 1 shows a schematic diagram of an oxide buildup versus time plots that can be noted during a typical electrochemical reaction.

From Figure 1, it can be understood that the electrochemical process initially occurs at a faster rate (i.e. Stage I). Next the kinetics proceeds at a slower rate (Stage II), and eventually the reaction precedes at a much slower pace (Stage III) or sometimes, the reaction show a trend that the reverse process is taking place.

During Stage I, the corrosion / electrochemical reaction proceeds at a faster rate as a result of unimpeded chemical reaction between metal and the corroding medium. Therefore, it can be assumed that during Stage I,

The overall chemical reaction rate at

Stage I (Fast oxide growth stage) $((dw/dt)_{\text{Stage I}} = A(w_1 / t_1)$ [2]

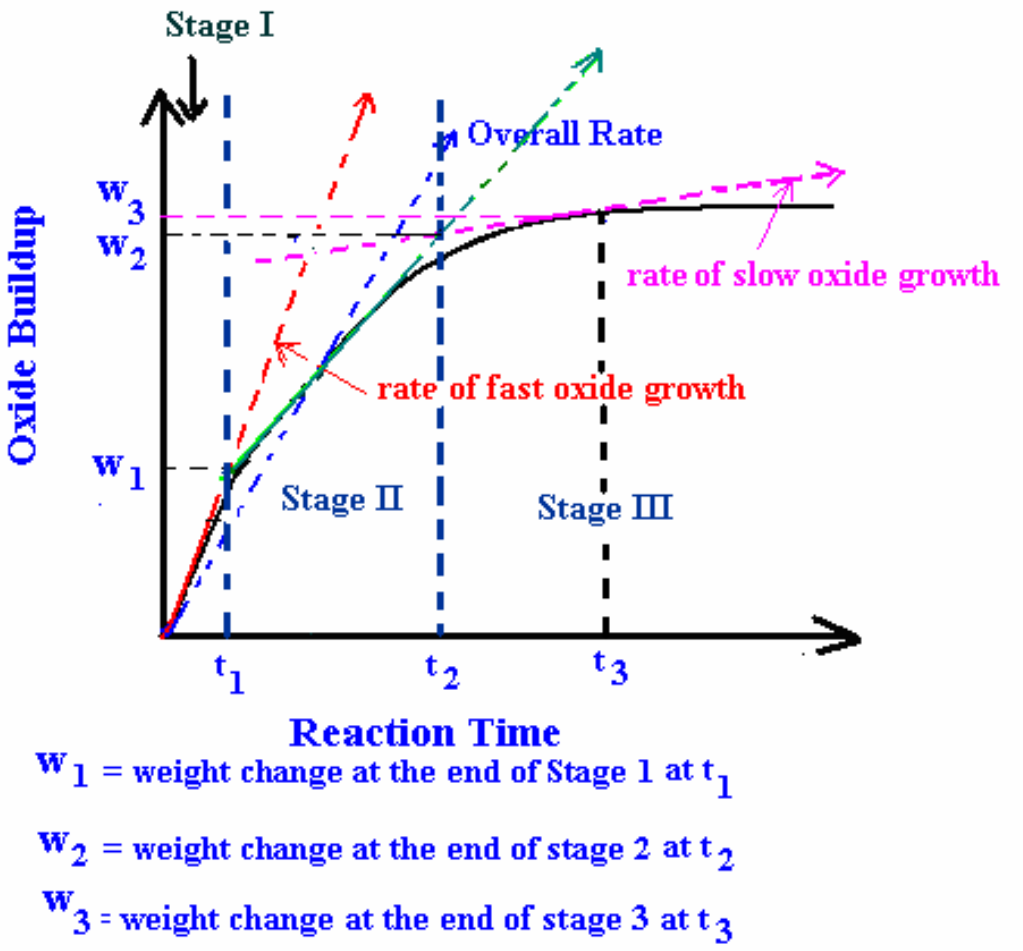

Figure 1. Schematic representation of the electrochemical reaction versus reaction time plots.

The Stage II reaction represents a transitional zone between the fast and slow chemical reaction (i.e. a chemical zone in which a fast reaction process (i.e. first stage) begins to slow down and the oxide build up begins at a slower pace). In many reactions, the transitional zone

may be small, so that this region can be ignored. However, for the process in which diffusion is important, the overall rate of reaction in Stage II is given as

$$\textbf{Stage II (Intermediate stage)} \quad (dw/dt)_{\text{Stage II}} = A\,(w_2 - w_1) / (t_2 - t_1) \qquad [3]$$

During Stage III, a slow and steady chemical reaction continues with time and a continuous build up of a third oxide at a slower reaction rate can be seen. Therefore, the overall rate of reaction in Stage III is given as

$$\textbf{Stage III (Slow oxide buildup stage)} \quad (dw/dt)_{\text{Stage III}} = A\,(w_3 - w_2) / (t_3 - t_2) \qquad [4]$$

In metallurgical processes such as the oxidation and reduction of metal alloys, the oxide growth imparts a steady effect on the electrical, mechanical, and or structural properties of the host metal. If the growth of oxide is uniform, the information (viz. electrical, mechanical and structural properties) obtained on the oxidized metal can be assumed to follow a kinetics of the oxidation process. For example, the rate of oxidation can be treated in terms of the normalized change in the structure or change in the mechanical properties or the electrical properties. Thus, the above relationships obtained for different stages can be rewritten as follows:

The overall rate chemical reaction ≈ rate of change in the structure of material at Stage I

$$\textbf{Stage I (Fast oxide growth stage)} \quad (dS/dt)_{\text{Stage I}} = B\,(S_1 / t_1) \qquad [5]$$

where B is a constant, and ‘S’ represents the normalized volume fraction and /or the area fraction of a newly formed structure as result of chemical reaction at time ‘t’.

The Stage II reaction represents a transition zone between the fast and slow chemical reaction (i.e. a chemical zone in which a fast reaction process (i.e. first stage) begins to slow down and the oxide buildup begins at a slower pace). It has to be emphasized that in many reactions, the transitional zone may be small, so that this region can be ignored.

The overall rate of reaction in Stage II is given as

$$\textbf{Stage II (Intermediate stage)} \; (dS/dt)_{\text{Stage II}} = B\,(S_2 - S_1) / (t_2 - t_1) \qquad [6]$$

During the third stage, a slow and steady chemical reaction continues with time and a continuous change in the structure of the host occurring at a slower reaction rate can be seen.

Therefore, the overall rate of reaction in Stage III is given as

$$\textbf{Stage III (Slow oxide buildup stage)} \quad (dS/dt)_{\text{Stage III}} = B\,(S_3 - S_2) / (t_3 - t_2) \qquad [7]$$

A similar transformation based on the measured electrical properties (such as the measured change in the potential) can be equated to the kinetic parameters as follows: As the electrochemical reaction is progressing at the solid liquid interface (corrosion at the metal - solution interface), and if one assumes that an oxide layer forms and grows uniformly covering the entire surface of the metal surface, a constant change in the potential corresponding to the oxide buildup also occurs. Thus the normalized change in the potential (potential measure with oxide film / the potential of the metal surface at the start of the electrochemical reaction) with time can be represented as:

$$(dV/dt) \propto -\{ (dV_{oxide}/dt) \} \text{ or } (dV/dt) = C\{ (dV_{oxide}/dt) \} \qquad [8]$$

where C is a constant and 'V' represents the normalized volume fraction and /or the area fraction of a newly formed structure as result of chemical reaction at time 't'.

Therefore, the overall chemical reaction rate at Stage I, Stage II, and Stage III can be given as:

$$\textbf{Stage I (Fast oxide growth stage)} \quad (dV/dt)_{\text{Stage I}} = C\,(V_1 / t_1) \qquad [9]$$

$$\textbf{Stage II (Intermediate stage)} \quad (dV/dt)_{\text{Stage II}} = C(V_2 - V_1) / (t_2 - t_1) \qquad [10]$$

$$\textbf{Stage III (Slow oxide buildup stage)} \quad (dV/dt)_{\text{Stage III}} = C(V_3 - V_2) / (t_3 - t_2) \qquad [11]$$

The above equations provide solutions for the rate of the oxide film growth and the magnitude of the film growth represents the severity of the corrosion. However, the rate parameter will not provide a detailed analysis of the type of the chemical reaction (viz. the number of components that are participating in the corrosion process, the nature of chemical reaction etc.).

For the oxide formation, an electrochemical reaction between the metal surface and the corroding medium (i.e. ammonia or seawater) must occur. Initially, the corroding liquid will not have any problem reacting with the metal. As the reaction continues, the oxide film may act as a barrier between the corroding medium and the un-reacted metal surface. This requires the diffusion of liquid through the oxide layer to reach the metal surface. If it is assumed that the

volume of the corroding solution is very high and the concentration remains independent of the electrochemical reaction time, the kinetic parameters that control the corrosion process are the concentration of the metal species, the diffusion coefficient for the liquid flow through the oxide layers and the time. At the beginning, more metal is exposed to the solution, hence, the oxide forms very fast and the rate of oxide growth is represented as $\mathbf{(dw_{fast\ oxide\ growth}/dt)}$. Once the metal surface is covered with oxide film, for the electrochemical reaction to continue, the corroding solution has to diffuse through the oxide layers and the rate of diffusion of this process is represented as $\mathbf{(dw_{diffusion}/dt)}$. Once considerable oxide is formed, the reaction kinetics slows down. This is because, the solution has to diffuse further into the oxide film to find new metal surface. Therefore, the oxide formation takes a longer time and the rate is very low. The slow rate of corrosion is represented as

$$\mathbf{(dw_{\ slow\ oxide\ growth}/dt)}.$$

The general characteristics of oxide that is formed at a faster rate will have oxide that is irregular, coarse, non-uniform, loose and have a porous morphology. The oxide that is dominated by the diffusion process will have a porous morphology while the oxide that forms slowly will have a dense and uniform microstructure. The oxide formed as a result of fast reaction kinetics and the diffusion will have severe oxide cracking similar to that of mud cracking while the oxide that formed slowly with a slow diffusion of liquid will have uniform oxide with fine pores.

In order to understand the chemistry of the process, the original reaction kinetics equation, Equation 1 can be rewritten in terms of fast oxide growth, diffusion controlled oxide growth, and slow oxide growth as follows:

$$\mathbf{(dw_{oxide}/dt) = (dw_{fast\ oxide\ growth}/dt) + (dw_{diffusion}/dt) + (dw_{slow\ oxide\ growth}/dt)} \quad [12]$$

During the chemical reaction, if the oxide is assumed to form primarily due to fast chemical reaction between the metal and the corroding liquid, and the time required for the diffusion of the liquid to find new metal surface is small, then the rate of oxide build due to diffusion and other rate of other processes can be ignored. Therefore the overall corrosion process can be rewritten as:

$$\mathbf{(dw_{oxide}/dt) = (dw_{fast\ oxide\ growth}/dt)} \quad [13]$$

Similarly, if the oxide formation requires the diffusion of solution (through the pores of oxide formed) to find new metal surface, then the rates of other processes can be ignored. Therefore the overall corrosion process can be represented as:

$$(dw_{oxide}/dt) = (dw_{diffusion}/dt) \quad [14]$$

If the oxide formation requires long chemical reaction time and the rate determining step is only the slow chemical reaction, the other faster chemical processes (viz. diffusion etc.) can be ignored. Therefore during this process, the overall corrosion process is given as:

$$(dw_{oxide}/dt) = (dw_{slow\ oxide\ growth}/dt) \quad [15]$$

If it is assumed that the corroding liquid concentration remains constant and only the concentration of the metal species change with time, the integrated form of the corrosion process kinetic rate equations are given in terms of concentration (c) of the reacting species as:

$$\ln\{(dc_1/dt_1) / (dc_2/dt_2)\} = - n \{ \ln(c_1) - \ln (c_2)\} \quad [16]$$

$$\text{or} \quad n = - [\ln\{(dc_1/dt_1) / (dc_2/dt_2)\} / \{ \ln(c_1) - \ln (c_2)\}] \quad [17]$$

where 'n' is the order of reaction, and 'c_1' and 'c_2'are the concentration of the reactants at time 't1' and 't2' and (dc_1/dt_1) and (dc_2/dt_2) are the slopes measured by drawing a tangent to the concentration versus time curves at ((t_1, c_1) and (t_2, c_2)} respectively. The value of n equals to 'one' means that the concentration of 'one species' is continuously changing with time while the value of n equals to two means that the concentration of two species are changing continuously. The value of 0.5 and 0 represents the chemical reaction that is controlled by the diffusion process and time dependent process respectively. A mixed value of 1.5 represents a chemical reaction in which the concentration of one species is changing continuously with the reaction time. In addition, the diffusion process also influences the chemical reaction.

Results and Discussion

Figures 2 - 3 show the measured potential (whose data is shown in Table 1 and 2 respectively,) plotted against the electrochemical reaction time for all nickel aluminum bronze samples. The results suggest that there is no specific trend in the behavior of the potential change versus the chemical reaction time. However, when the same open circuit potential (OCP) data was plotted as a function of normalized change in the open circuit potential versus the electrochemical reaction time some meaningful patterns were observed. Figures 4 – 11 shows the normalized potential versus reaction time plots for all 16 samples whose data is obtained from Table 1 and 2 respectively. For normalization process the initial potential measure at (t=0) is taken as the base metal potential. As the electrochemical reaction is continued, the measured potential at any given time is taken as the potential that represents the metal and oxide film

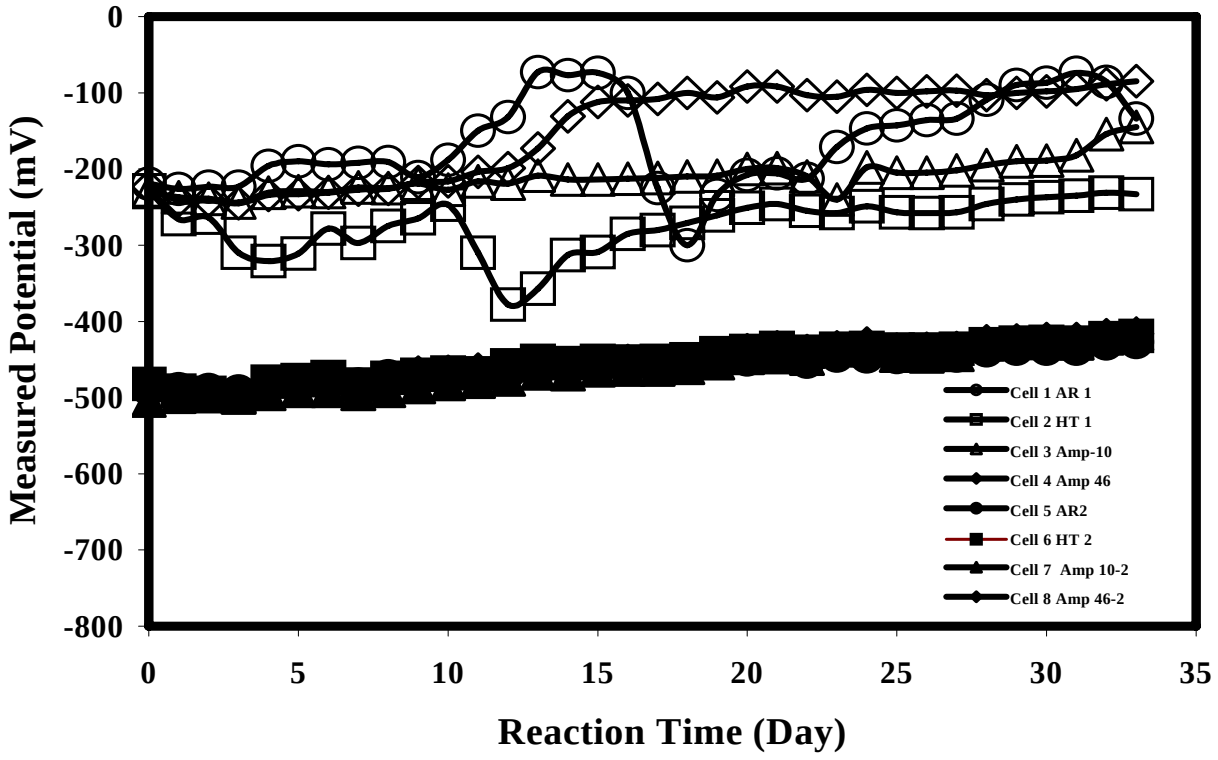

Figure 2. Normalized change in the potential (%) (versus SCE) versus reaction time profiles for nickel aluminum bronze samples treated with either seawater or ammonia solutions.

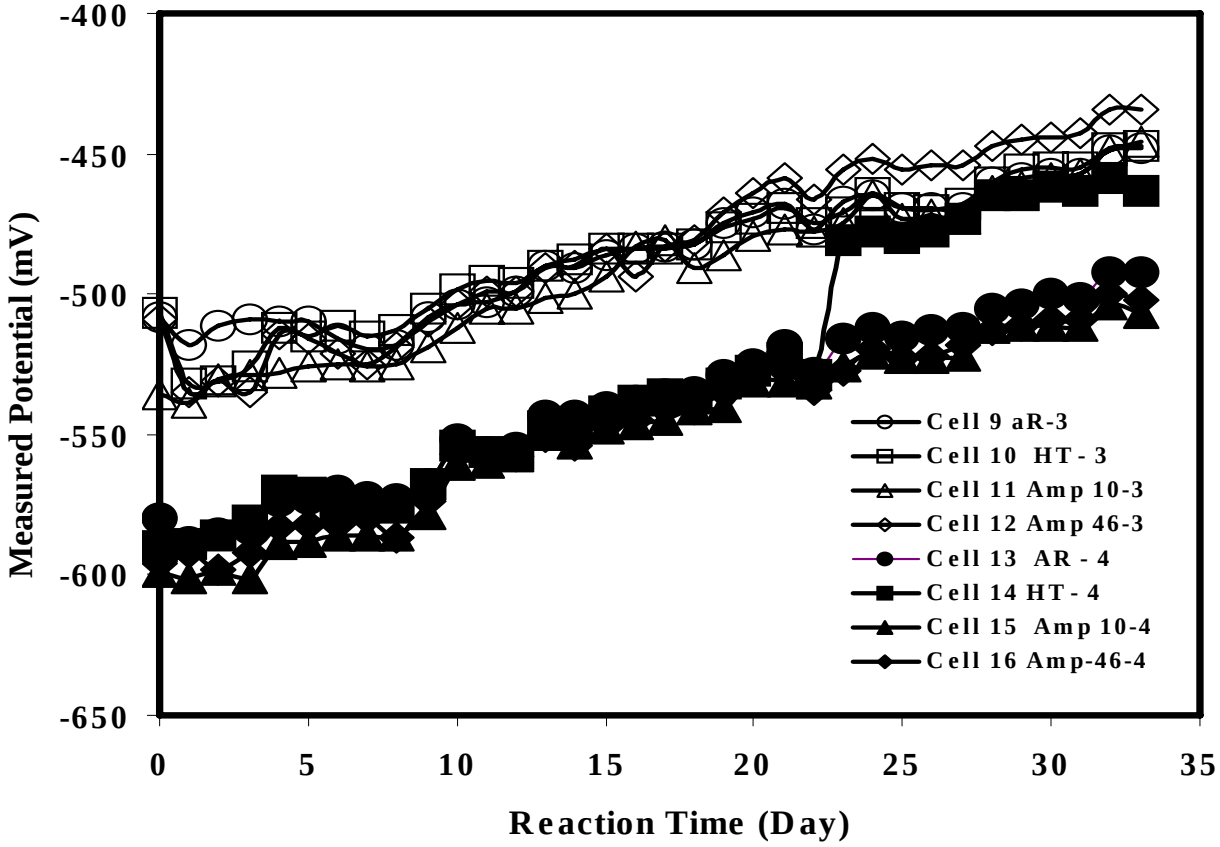

Figure 3. Normalized change in the potential (%) (versus SCE) versus reaction time profiles for nickel aluminum bronze samples treated with either seawater or ammonia solutions.

Table 1. Open circuit potentials (versus SCE) obtained for nickel aluminum bronze samples after exposure in seawater and 10% ammonia Solution respectively.

	Seawater				**10 % Ammonia**			
Reaction Time (Days)	Cell 1 AR1	Cell 2 HT1	Cell 3 Amp10	Cell 4 Amp46	Cell 5 AR2	Cell 6 HT2	Cell 7 Amp10-2	Cell 8 Amp46-2
0	-219	-228	-230	-223	-488	-482	-504	-492
1	-226	-266	-237	-241	-489	-491	-499	-497
2	-223	-264	-239	-241	-490	-494	-498	-496
3	-223	-310	-244	-245	-492	-498	-500	-499
4	-196	-321	-231	-234	-481	-479	-495	-485
5	-190	-311	-229	-233	-481	-477	-491	-481
6	-194	-278	-230	-231	-480	-473	-491	-487
7	-192	-297	-224	-227	-483	-483	-495	-483
8	-191	-275	-225	-226	-472	-474	-491	-478
9	-211	-265	-219	-217	-470	-470	-486	-467
10	-188	-247	-227	-216	-471	-467	-482	-466
11	-150	-310	-216	-204	-468	-468	-479	-463
12	-132	-378	-219	-199	-467	-458	-476	-463
13	-73	-357	-209	-173	-464	-452	-468	-458
14	-77	-313	-214	-131	-462	-455	-469	-457
15	-74	-309	-214	-112	-460	-452	-464	-454
16	-100	-285	-213	-110	-460	-453	-463	-452
17	-225	-280	-212	-108	-459	-452	-463	-453
18	-300	-271	-210	-100	-459	-450	-461	-457
19	-234	-261	-209	-106	-452	-442	-455	-443
20	-208	-251	-200	-92	-450	-439	-448	-438
21	-206	-246	-199	-92	-444	-435	-447	-434
22	-213	-255	-210	-103	-453	-440	-449	-439
23	-171	-258	-240	-105	-445	-436	-435	-434
24	-147	-249	-198	-96	-446	-435	-438	-429
25	-143	-257	-205	-100	-447	-437	-445	-437
26	-136	-258	-205	-98	-445	-437	-446	-436
27	-134	-257	-202	-97	-445	-436	-444	-435
28	-109	-246	-195	-103	-438	-430	-430	-426
29	-90	-240	-190	-100	-436	-428	-428	-425
30	-87	-237	-189	-98	-436	-427	-428	-423
31	-74	-235	-182	-95	-436	-428	-429	-423
32	-86	-231	-154	-89	-429	-422	-422	-418
33	-134	-233	-145	-85	-427	-419	-416	-416

Table 2. Open circuit potentials (versus SCE) obtained for nickel aluminum bronze samples after exposure in 20% and 50% ammonia solution respectively.

	20 % Ammonia				50 % Ammonia			
Reaction Time (Days)	Cell 9 AR-3	Cell 10 HT-3	Cell 11 Amp10-3	Cell 12 Amp46-3	Cell 13 AR-4	Cell 14 HT-4	Cell 15 Amp10-4	Cell 16 Amp-46-4
0	-508	-507	-536	-509	-580	-590	-599	-596
1	-518	-532	-539	-535	-588	-589	-601	-592
2	-511	-531	-530	-531	-585	-586	-598	-598
3	-509	-526	-529	-535	-584	-581	-601	-592
4	-510	-512	-528	-514	-574	-570	-589	-583
5	-510	-515	-526	-516	-573	-571	-588	-582
6	-516	-511	-525	-521	-570	-576	-586	-582
7	-520	-515	-526	-525	-572	-575	-586	-580
8	-518	-513	-525	-519	-573	-576	-586	-587
9	-508	-505	-519	-510	-568	-568	-578	-574
10	-504	-498	-512	-504	-552	-554	-561	-557
11	-503	-495	-505	-499	-556	-556	-560	-559
12	-499	-496	-505	-499	-555	-557	-558	-558
13	-490	-490	-501	-491	-543	-547	-550	-551
14	-491	-488	-500	-490	-543	-547	-553	-554
15	-486	-484	-494	-484	-540	-542	-548	-547
16	-484	-484	-483	-494	-538	-538	-546	-545
17	-483	-484	-481	-483	-536	-536	-545	-541
18	-482	-482	-491	-481	-535	-537	-541	-541
19	-475	-476	-486	-471	-529	-532	-540	-535
20	-471	-473	-479	-464	-525	-527	-531	-530
21	-468	-469	-477	-459	-518	-523	-531	-527
22	-477	-475	-478	-466	-528	-529	-532	-534
23	-467	-471	-475	-456	-516	-481	-526	-527
24	-465	-464	-465	-452	-512	-478	-521	-520
25	-469	-469	-473	-456	-515	-480	-523	-523
26	-469	-470	-472	-454	-513	-478	-523	-522
27	-469	-468	-473	-454	-512	-473	-522	-518
28	-460	-460	-463	-447	-505	-465	-512	-513
29	-459	-456	-462	-445	-504	-465	-511	-511
30	-457	-455	-459	-444	-500	-462	-511	-509
31	-457	-455	-457	-443	-501	-463	-511	-509
32	-449	-448	-449	-434	-492	-459	-504	-500
33	-448	-447	-446	-434	-492	-463	-507	-502

The normalized potential (%) versus reaction time plots (Figures 4 - 11) indicates that the initial reaction, (i.e. reaction during the first 7 - 10 days) is not smooth and the measured potential values show significant scatter in the data. It is possible that the initial reaction phase represents a non-equilibrium situation and/or a reaction in which the reactants (viz. copper, nickel, aluminum, iron etc.) do not participate in the electrochemical reaction at the same rate and time. For example, it is well known that the ammonia forms a number of different metal ammonium complexes (with copper, nickel, iron), and the compound formation depends upon the chemical reactivity, the ionic strength, and ion concentration. The chemical composition (and *structure*) of these complexes change (or *rearrange*) with time in order to form one or more stable compounds. The seawater has a chloride ion concentration and during the electrochemical reaction, the metal chloride will also form and deposit on the metal surface. Since this is a first attempt to check whether an electrochemical process in which only OCP data is available can be tested for the reaction kinetics model and successfully predict the oxide properties. The OCP data from day 10 till day 33 were considered for modeling. The results also indicate that the chemical reaction behavior for NAB samples tested in cell 1- 16 can be classified into 3 different categories. The first two samples that were reacted with seawater had no correlation. It is possible that the variation in measured data represent samples whose oxide layers broke and fell into the solution. The samples in test cells 3 and 4 show an accelerated oxide zone followed by slow reaction zone and a sudden increase in the oxide buildup. This may be due to the formation of a second type of oxide that required a longer induction period. The other samples within experimental error showed rapid oxide growth followed by a slow down in the chemical reaction

Assuming that the NAB corrosion required 10 days of induction period, the normalized potentials from day 10 to day 33 were plotted as a function of time. All the samples that were exposed to 10 or 20% ammonia showed two reaction zones or stages ((i). fast oxide growth stage and (ii). slow oxide buildup stage) only. Figure 12 shows a typical plot of normalized potential change versus reaction time for NAB sample exposed to 20% solution. The NAB samples exposed seawater (cells 3 and 4), and 50% ammonia (Cells 13, 14, 15 and 16) also showed three distinguishable reaction zones (viz. (i) fast oxide growth region, (ii) intermediate stage and (iii) slow oxide buildup stage).

The rate of the reaction and the order of reaction for the overall process from day 10 onwards were determined by drawing tangents for the normalized voltage change versus reaction time plots at two concentrations and determining the slopes at those two concentrations. Similarly, the order of reaction for a given stage was determined by taking the slope at two concentrations within the limits of that stage.

Table 3 provides the kinetic parameters obtained for all NAB samples determined from the OCP data. The results suggest that electrochemical reaction of NAB in 10 and 20% ammonia is similar. However, the rate of reaction in 20% ammonia is slightly higher than in 10% ammonia solution. The overall electrochemical reaction in both cases (NAB-10 and 20% ammonia) is diffusion controlled and the NAB concentration determines the chemical reaction during first stage. The slow oxide build up stage is a time dependant process. The overall chemical reaction of NAB – seawater and NAB-50% ammonia system controlled both by diffusion process and the change in the metal concentration. The first stage is controlled by the change in NAB concentration. The intermediate stage is a time dependent process, which is followed by a complex chemical reaction in which several reactants are actively participating.

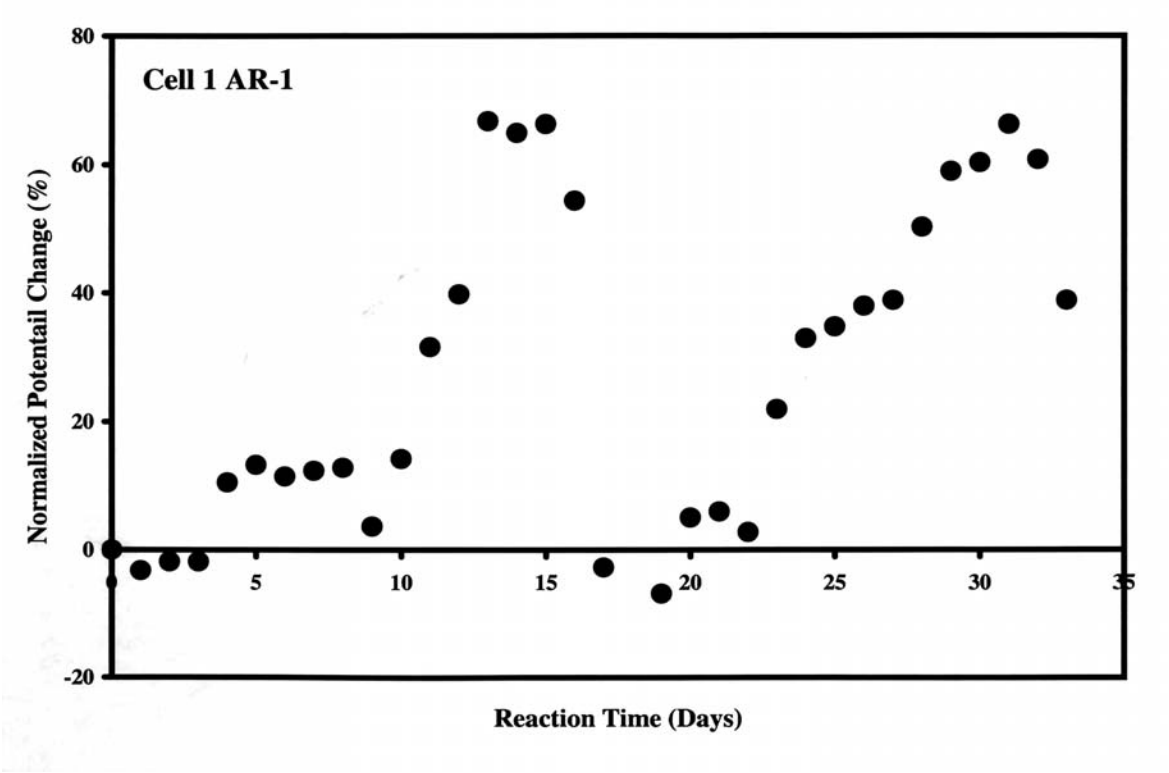

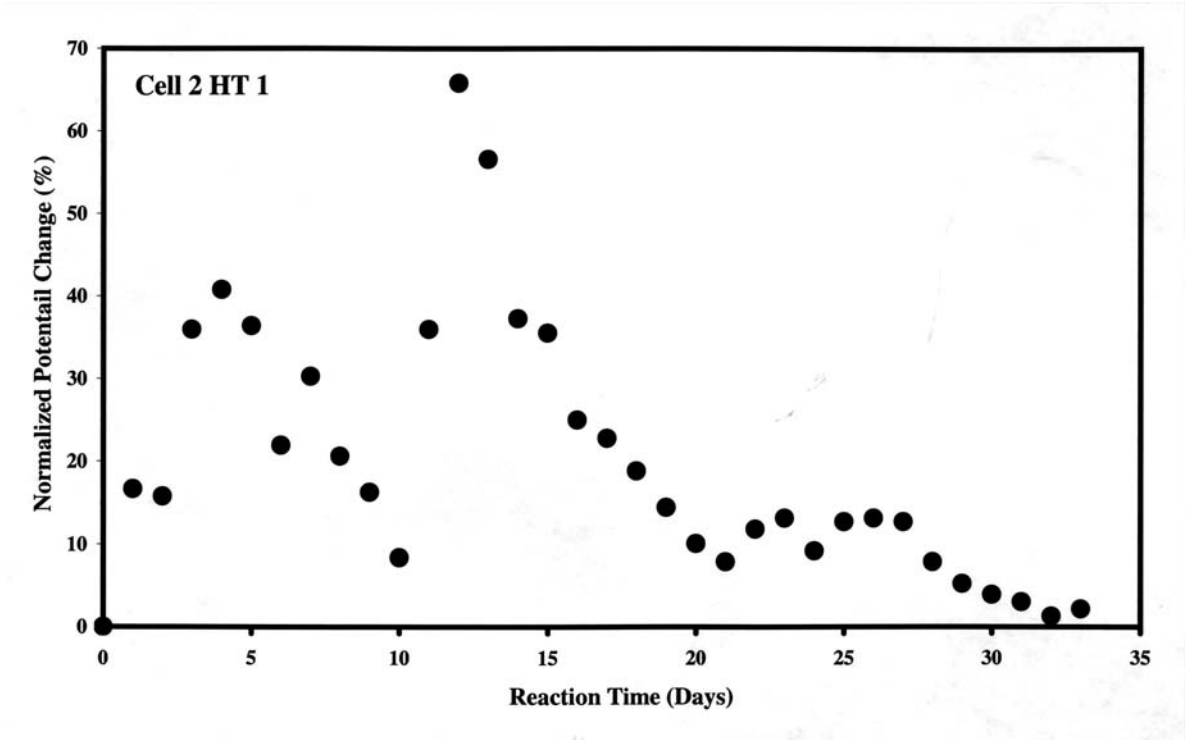

Figure 4. Normalized potential change (%) (versus SCE), versus reaction time for nickel aluminum bronze sample reacted with seawater.

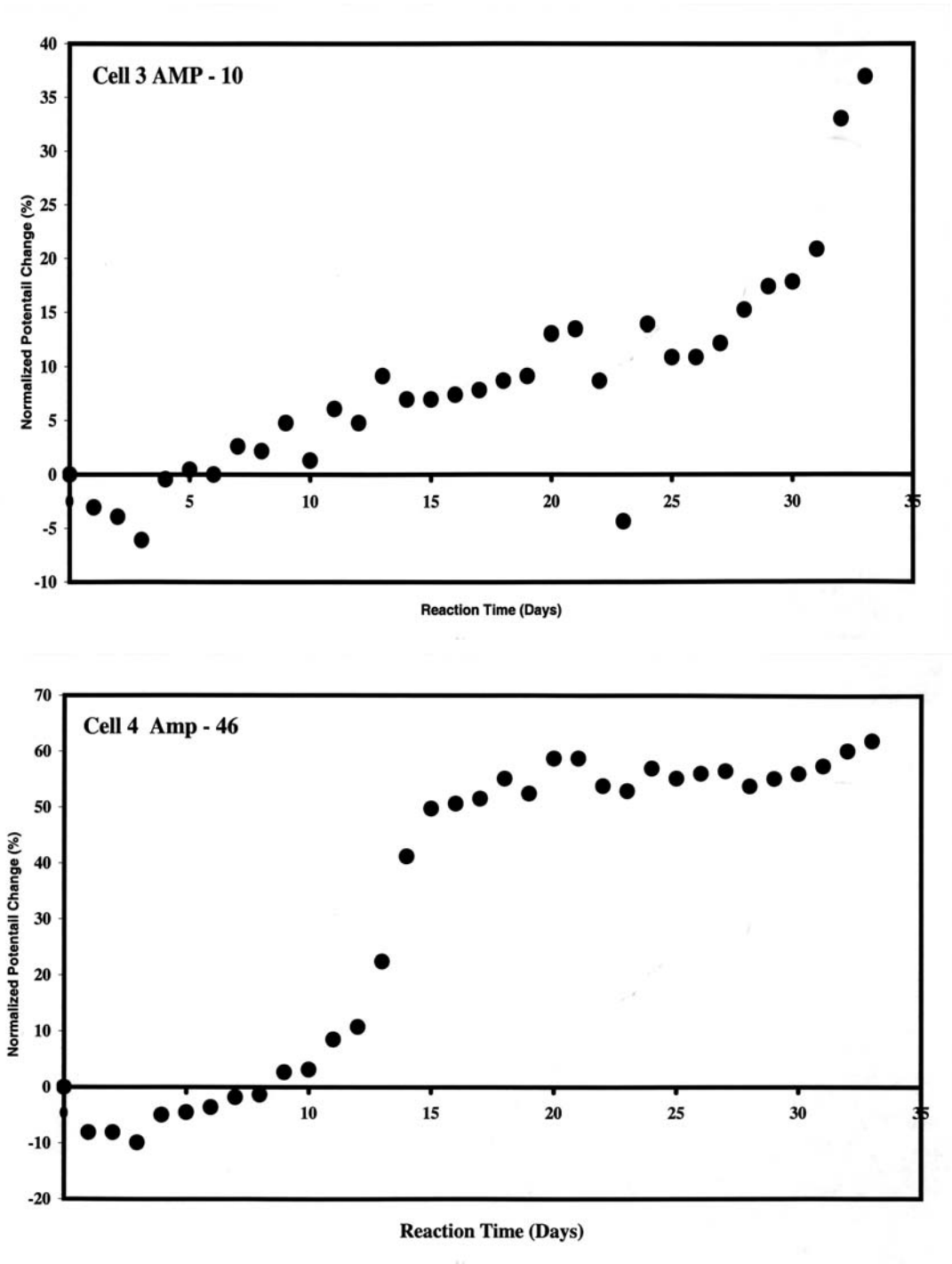

Figure 5. Normalized potential change (%) (versus SCE), versus reaction time for nickel aluminum bronze sample reacted with sea water

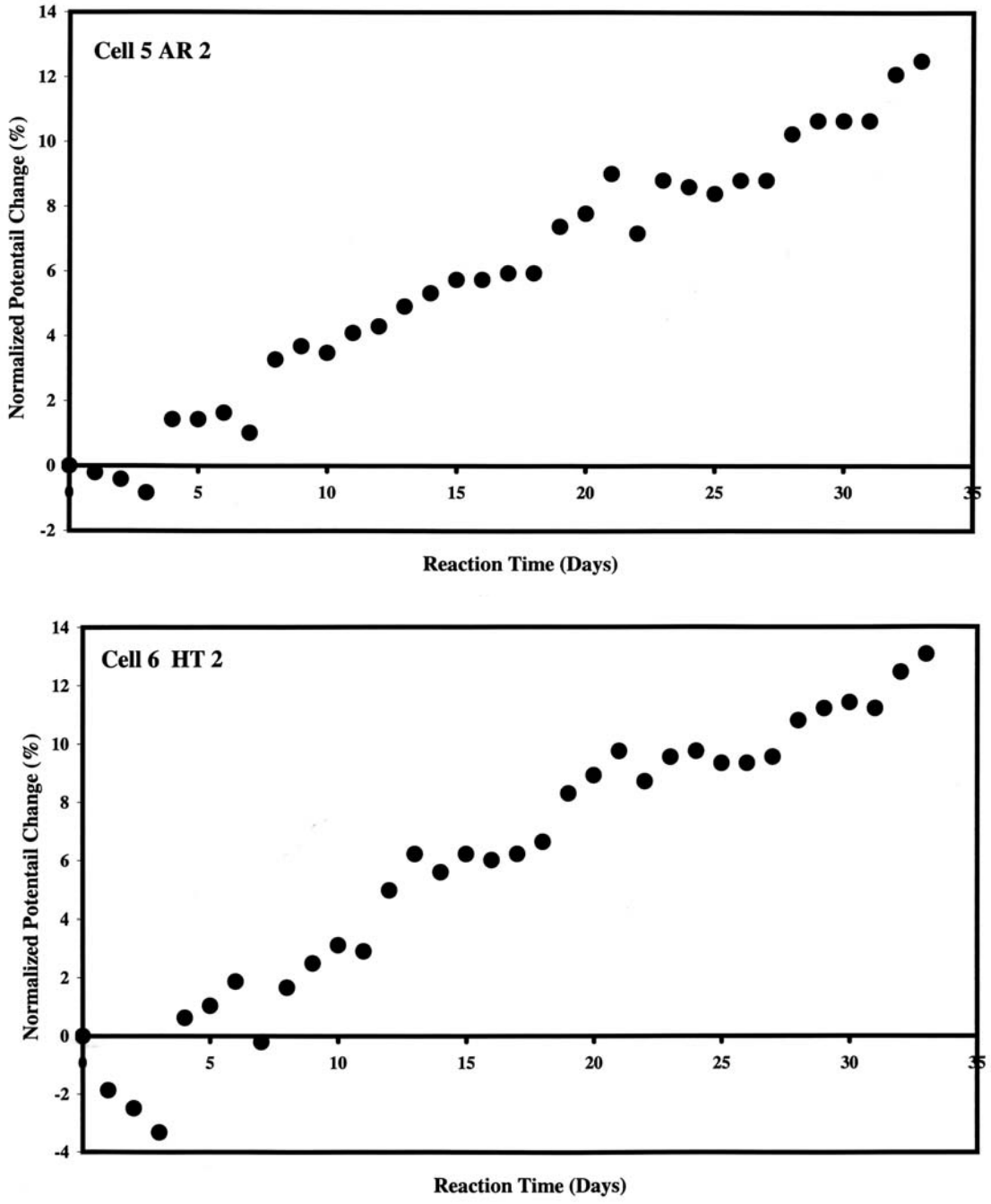

Figure 6. Normalized potential change (%) (versus SCE), versus reaction time for nickel aluminum bronze sample reacted with 90% water - 10% ammonia solution.

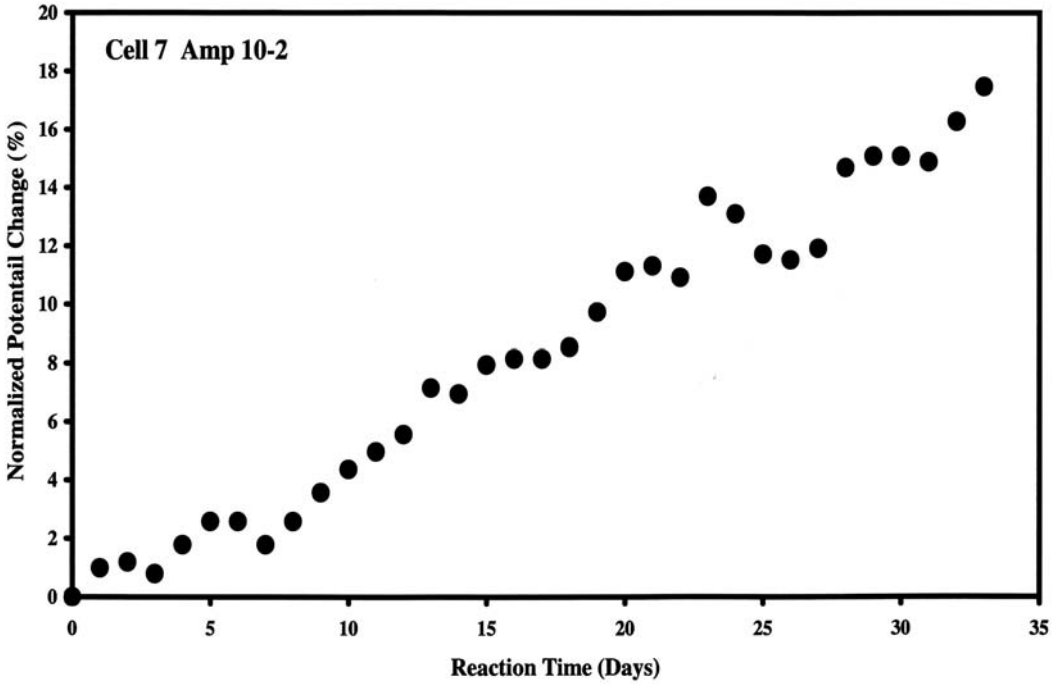

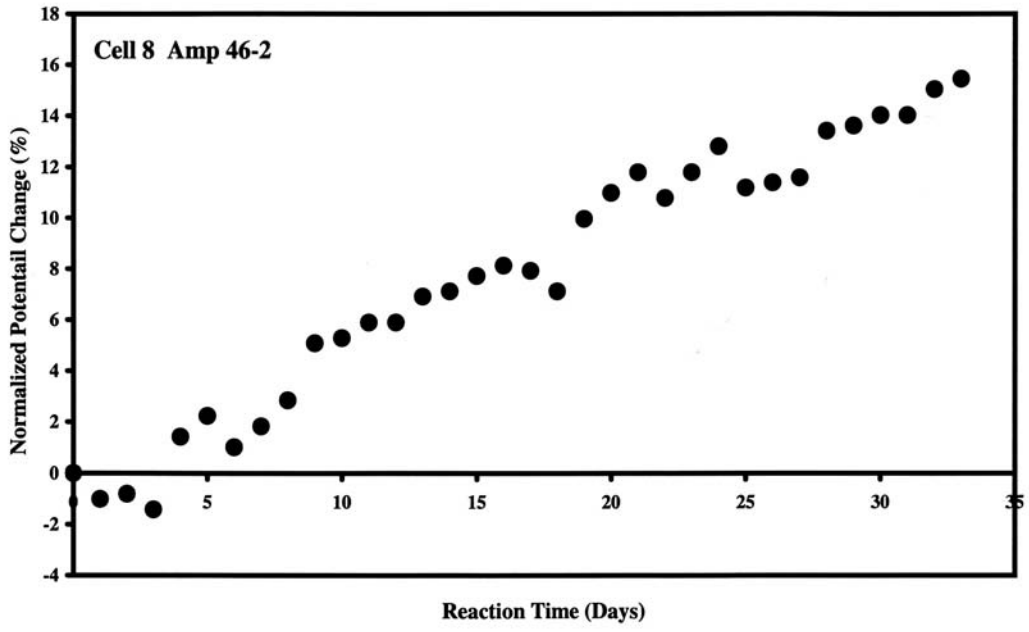

Figure 7. Normalized potential change (%) (versus SCE), versus reaction time for nickel aluminum bronze sample reacted with 90% water - 10% ammonia solution.

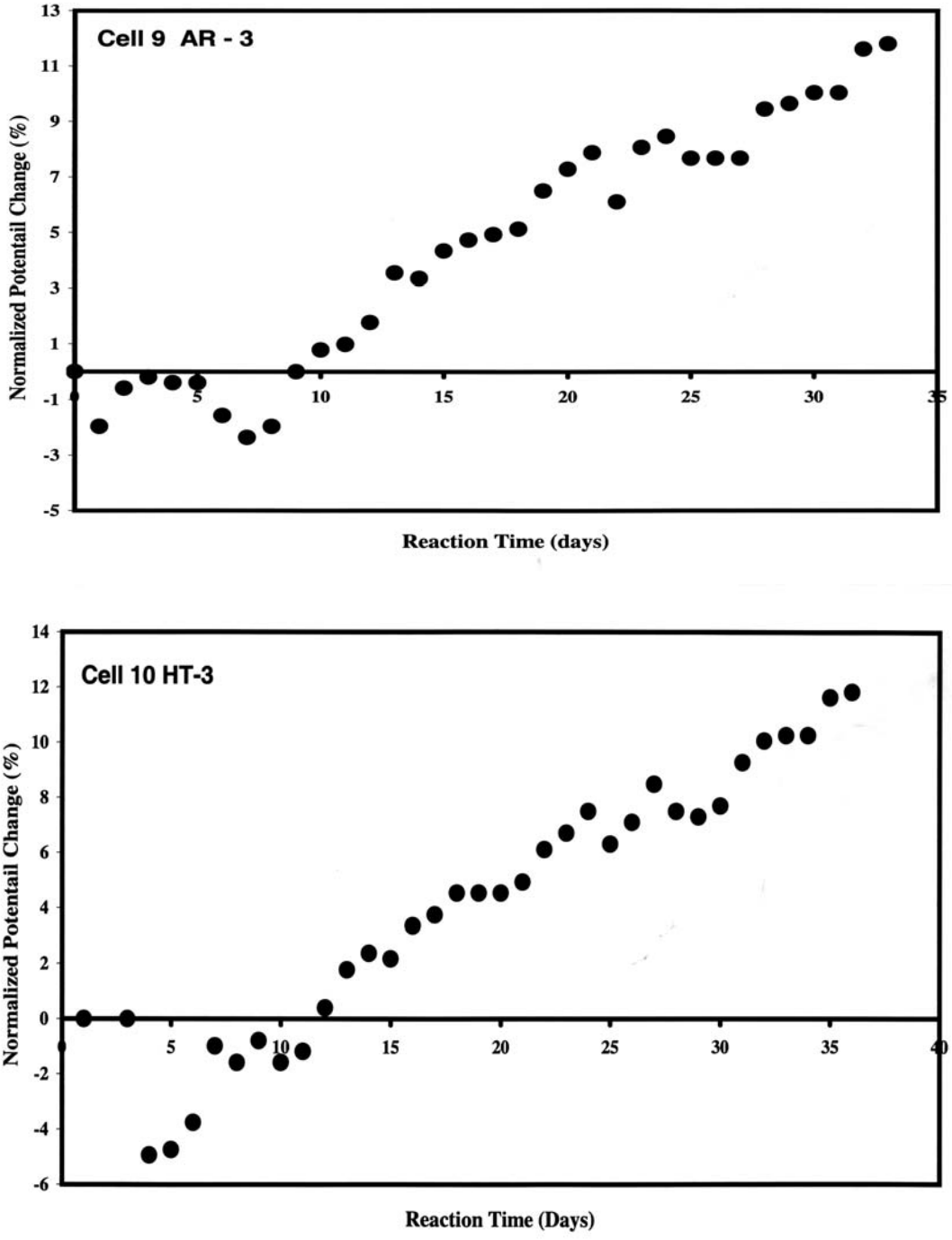

Figure 8. Normalized potential change (%)(versus (SCE) versus reaction time for nickel aluminum bronze sample reacted with 80% water - 20% ammonia solution.

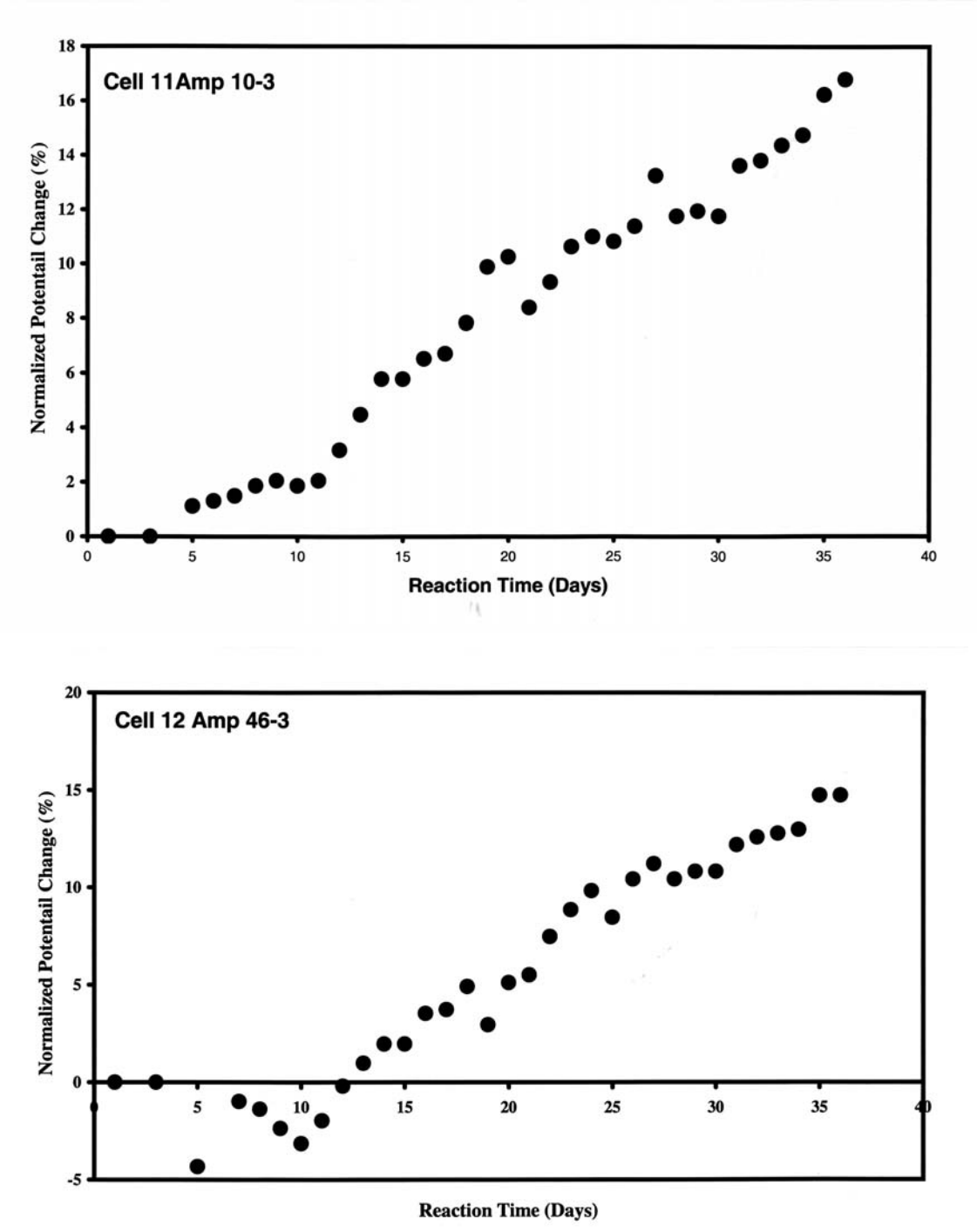

Figure 9. Normalized potential change (%)(versus (SCE) versus reaction time for nickel aluminum bronze sample reacted with 80% water - 20% ammonia solution.

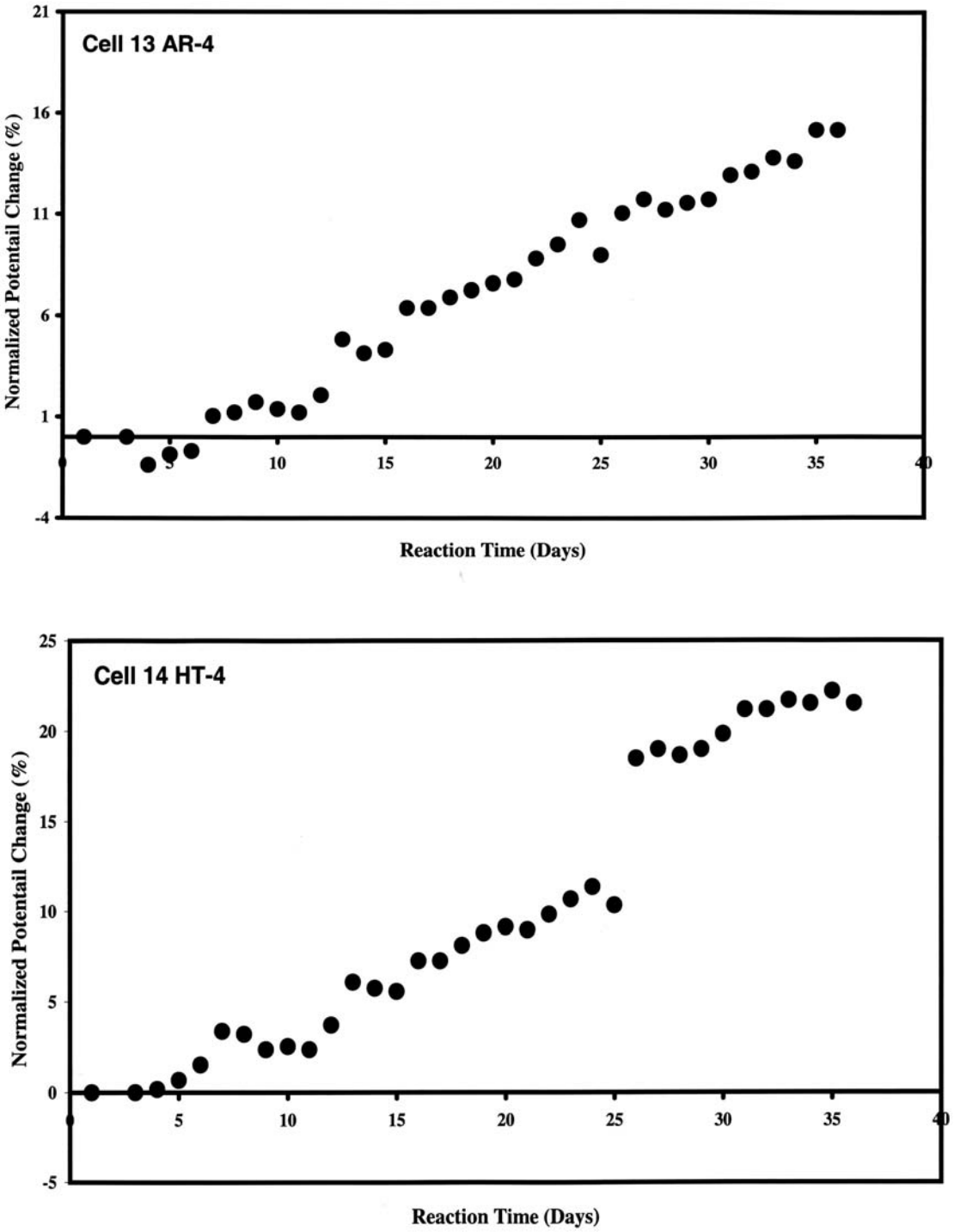

Figure 10. Normalized potential change (%)(versus (SCE) versus reaction time for nickel aluminum bronze sample reacted in 50% water - 50% ammonia solution.

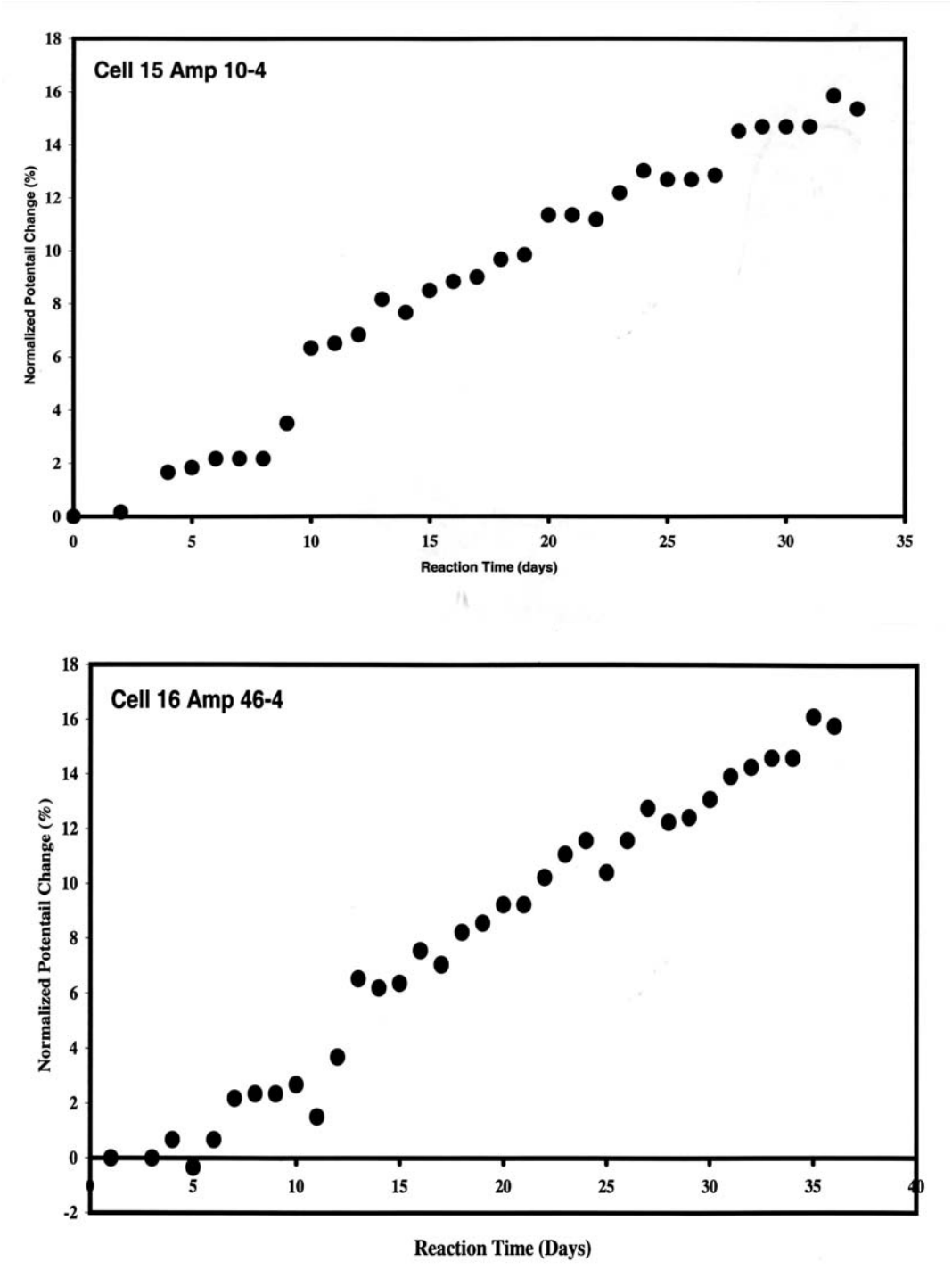

Figure 11. Normalized potential change (%)(versus (SCE) versus reaction time for nickel aluminum bronze sample reacted in 50% water - 50% ammonia solution.

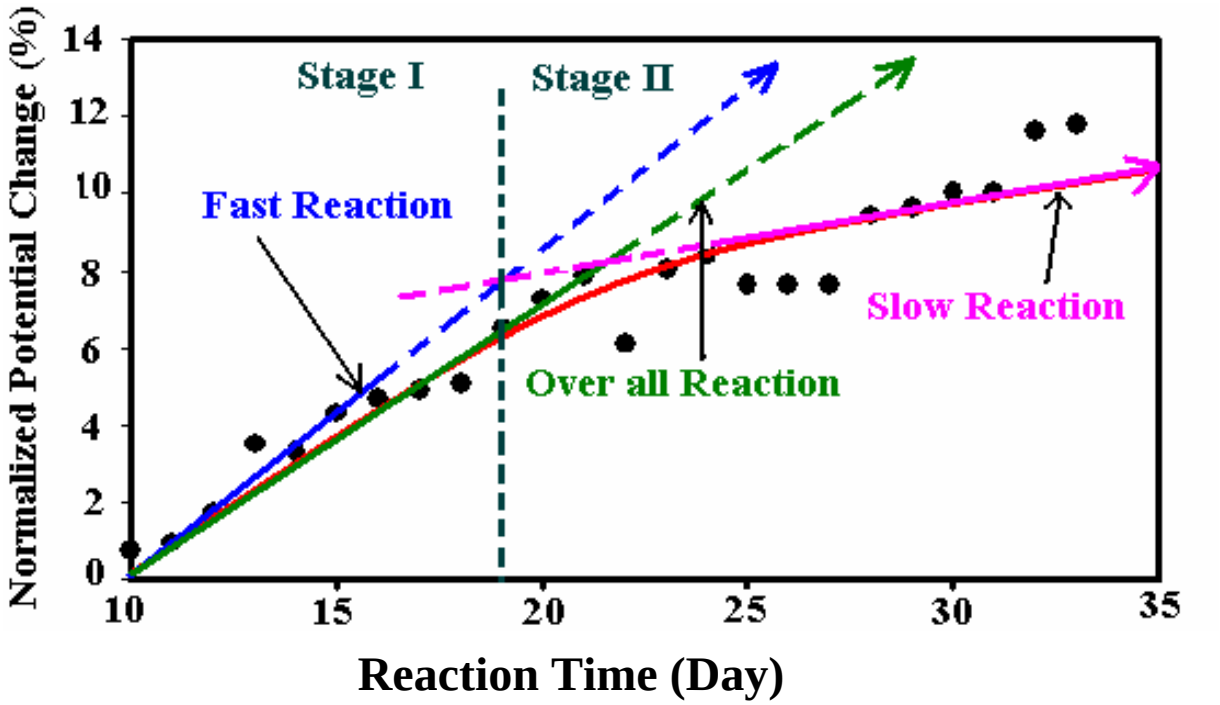

Figure 12. Normalized potential change (%) (versus SCE), versus reaction time plot of nickel aluminum bronze Sample treated in 80% water - 20% ammonia solution. The Figure also illustrates different stages of reaction and different tangents drawn to determine rate constants.

The chemical kinetic results for the NAB exposed to ammonia solution show that a diffusing process influences the overall chemical reaction kinetics. Therefore, it is reasonable to suggest that the oxide layer is associated with some degree of porosity. In addition, the results for NAB in 50% ammonia also indicate that the metal concentration continuously changes during the first stage. This means that during the oxide buildup, the liquid has to diffuse at a faster rate to find new metal surface. Such a process would produce cracking of the oxide layers and the net result would be the formation of a porous oxide surface with considerable 'mud cracking'. Therefore, the morphology of the oxide formed for the NAB samples will not be uniform and the surface topography changes significantly at different regions of the sample surface. The results for NAB – Seawater suggest that diffusion plays an active role during the entire corrosion process.

The second experimental analysis was carried out on the data obtained for nickel, 90-10 and 70-30 copper nickel alloys reacted with either KOH [3] and /or simulated sea water [2,3] at different constant positive or negative potential for over 24 hours. The data collected were the

information on the change in structure as a function of time using x-ray diffraction (Figures 13 - 20). Figures 13 and 14 are the x-ray diffraction patterns obtained for nickel in KOH samples undergoing electrochemical reduction at - 800 mV (versus SCE) and +450 mV (versus SCE) respectively. The results shown in Figures 13 and 15 were obtained during a cathodic reaction, and the results in Figures 14 and 16 represent the change in structure of nickel foil during the electrochemical anodic reaction respectively.

Table 3. Kinetic parameters determined from normalized open circuit potentials (versus SCE) obtained for nickel aluminum bronze samples after exposure to sea water, 10%, 20% and 50 % Ammonia Solution respectively.

Cell No	Sample ID	Over all Process		Stage I (Fast Growth)		Stage II (Slow Growth) / (Intermediate)		Stage III (Fast Growth)/ (Slow Growth)	
		Reaction Rate (k) (%/day)	*Order* (n)	Reaction Rate (k_1) (%/day)	*Order* (n_1)	Reaction Rate (n_2) (%/day)	*Order* (n_2)	Reaction Rate (k_3) (%/day)	*Order* (n_3)
1	AR1								
2	HT 1								
3	Amp10	0.62	*1.5*	0.83	*1.0*	0.52	*0.5*	5.0	*1.5*
4	Amp46	7.7	*1.5*	9.3	*1.0*	0.72	*0.5*	1.75	*1.0*
5	AR 2	0.5	*0.5*	0.6	*1.0*	0.29	*0*		
6	HT 2	0.56	*0.5*	0.68	*1.0*	0.35	*0*		
7	Amp 10-2	0.56	*0.5*	0.8	*1.0*	0.45	*0*		
8	Amp 46-2	0.73	*0.5*	0.9	*1.0*	0.46	*0*		
9	AR - 3	0.45	*0.5*	0.77	*1.0*	0.35	*0*		
10	HT - 3	0.45	*0.5*	0.76	*1.0*	0.38	*0*		
11	Amp 10-3	0.57	*0.5*	0.8	*1.0*	0.4	*0*		
12	Amp 46-3	0.72	*0.5*	0.82	*1.0*	0.41	*0*		
13	AR -4	0.75	*1.5*	1.1	*1.0*	0.57	0	0.35	*2.5*
14	HT – 4*	0.9		1.45	*0.5*	0.39	0		
15	Amp 10-4	0.54	*1.5*	0.68	*1.0*	0.52	0	0.37	*2.5*
16	Amp 46-4	0.56	*1.5*	0.9	*1.0*	0.52	0	0.36	*2.5*

HT – 4* ➔ Stage IV Reaction Rate (k_4) =0.55 %Oxide Growth per day, Order of the reaction (n_4) = 0

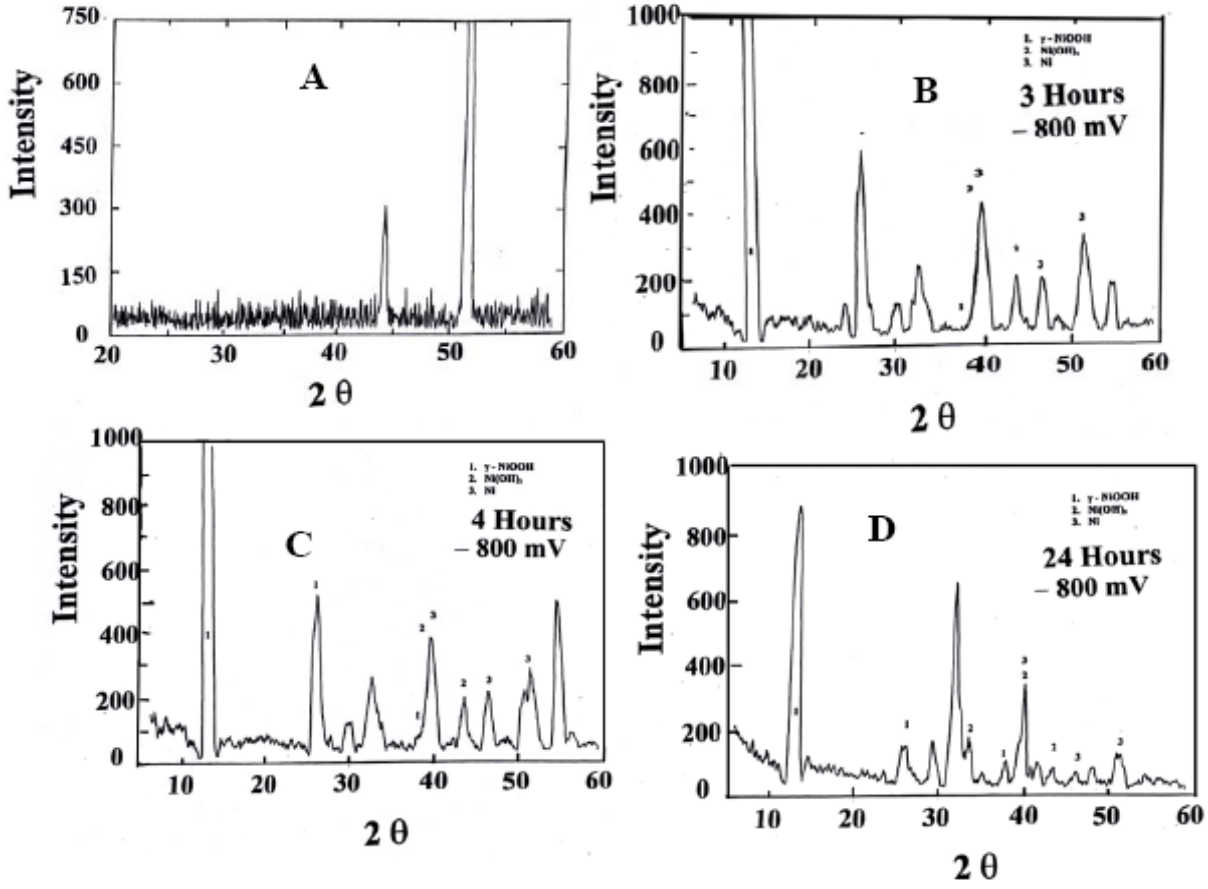

Figure 13. x-ray diffraction patterns obtained from nickel foil subjected to the electrochemical reaction at -800 mV (versus Ni/NiO electrode) in 5 M KOH solution. Reaction time (A) 0, (B) 3, (C) 4 and (D) 24 hours respectively.

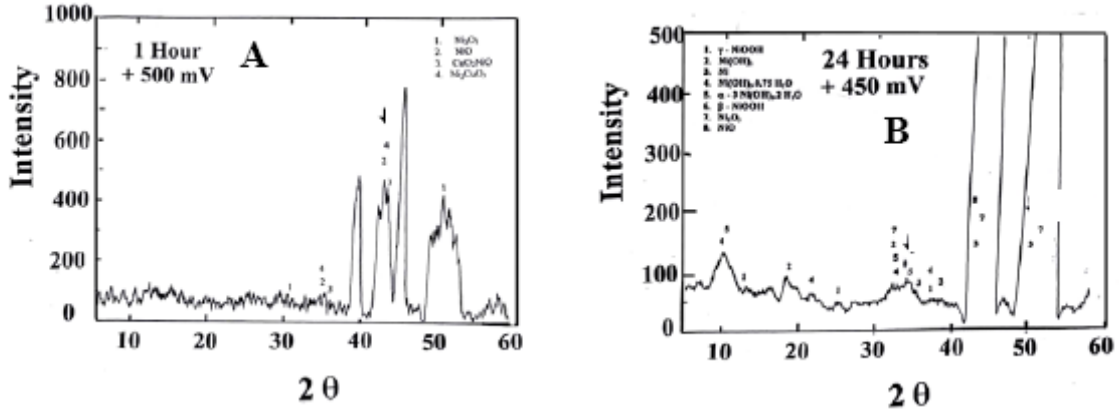

Figure 14: x-ray diffraction patterns obtained from nickel foil subjected to the electrochemical reaction at +450 mV (versus Ni/NiO electrode) mV in 5 M KOH solution. Reaction time (A) 0, and (B) 24 hours respectively.

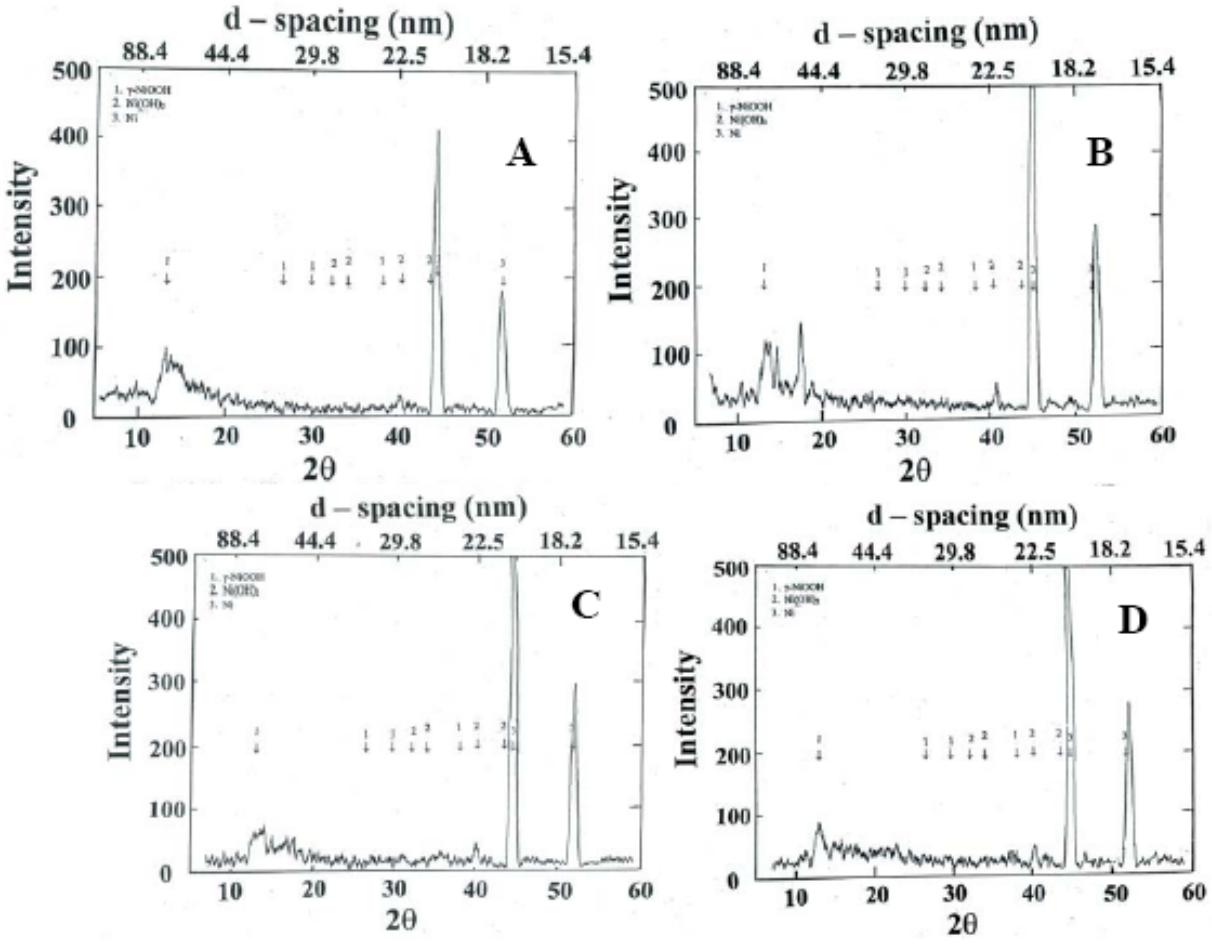

Figure 15. x-ray diffraction patterns obtained from nickel foil subjected to the electrochemical reaction at -800 mV (versus Ni/NiO electrode) in seawater. Reaction time (A) 0.5, (B) 2, (C) 4 and (D) 24 hours respectively.

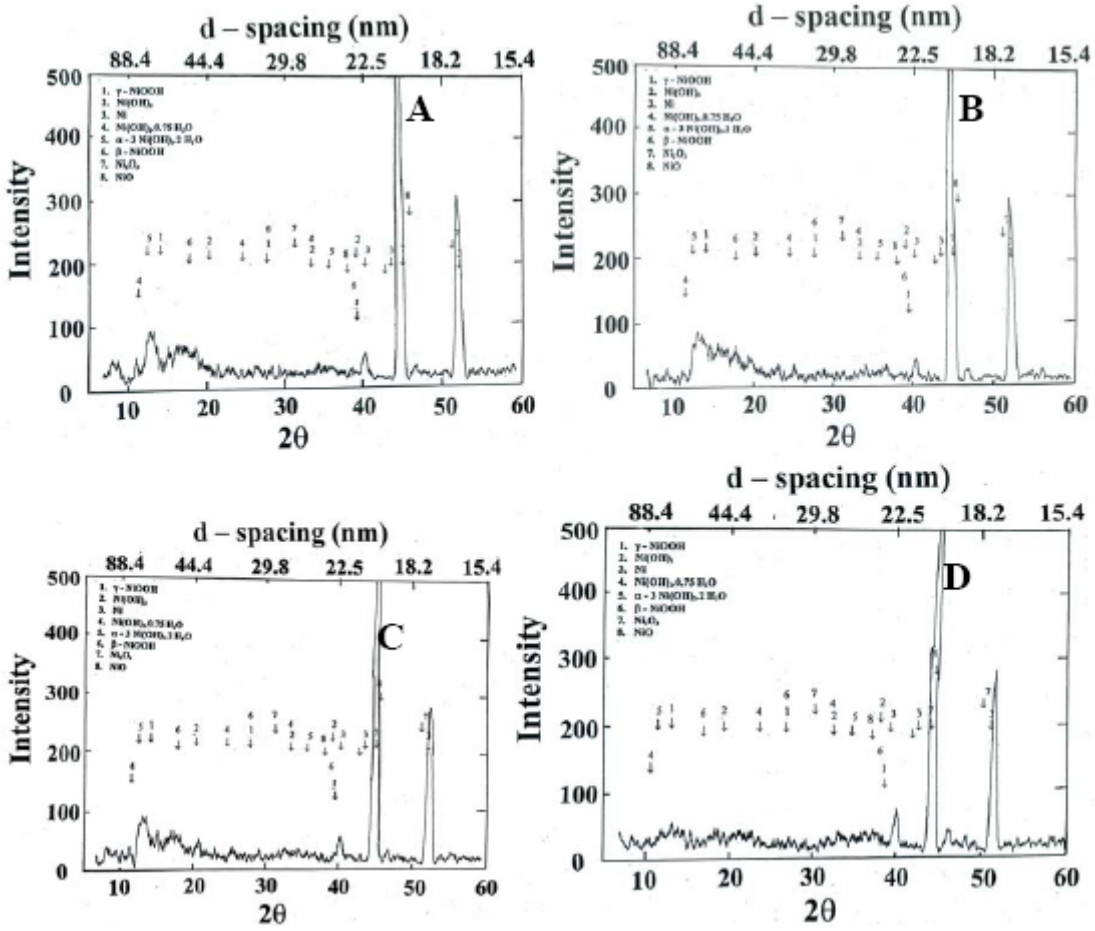

Figure 16. x-ray diffraction patterns obtained from nickel foil subjected to the electrochemical reaction at +450 mV (versus Ni/NiO electrode) in seawater. Reaction time (A) 0.5 , (B) 2, (C) 4 and (D) 24 hours respectively.

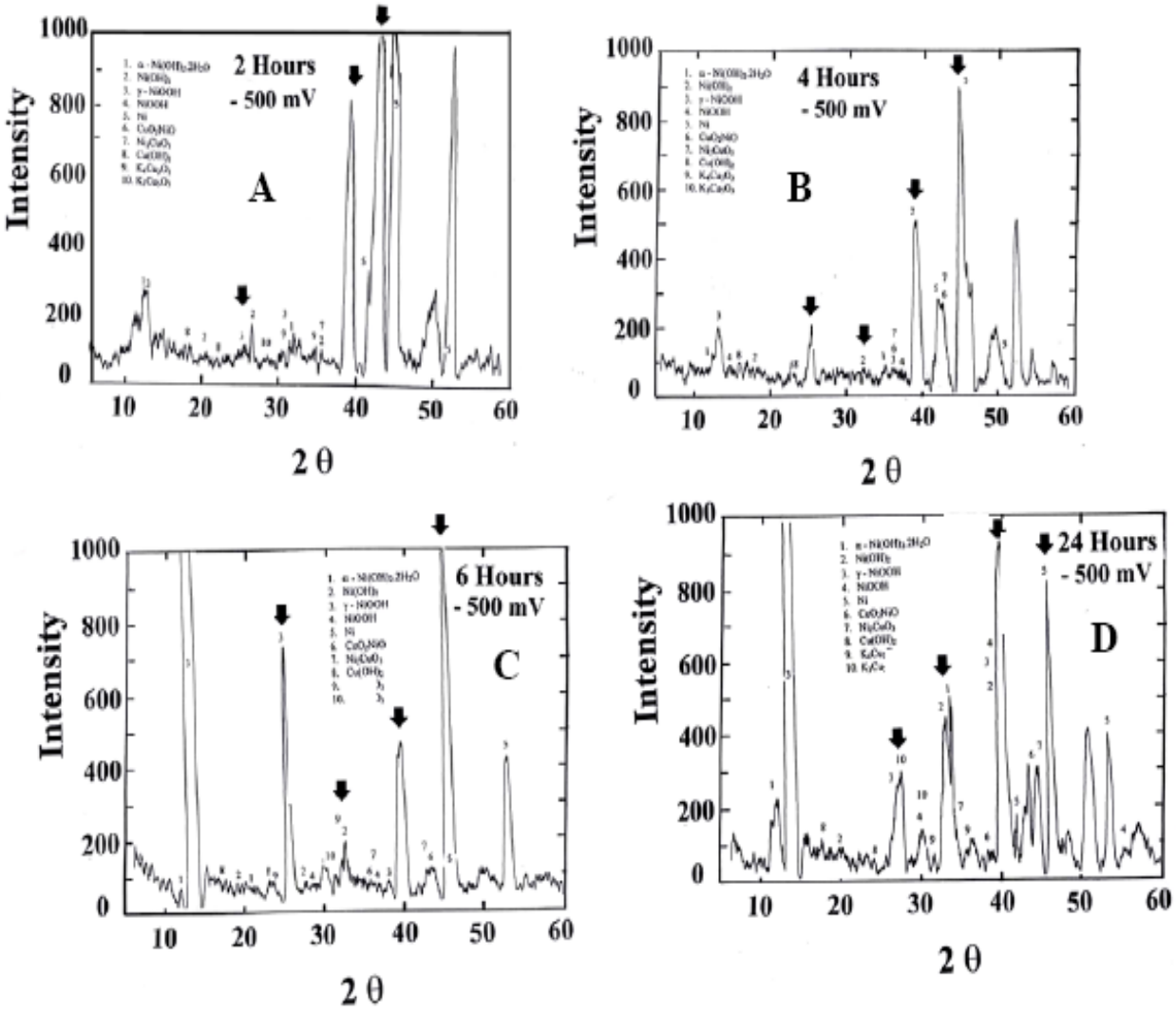

Figure 17. x-ray diffraction patterns obtained from 90-10 copper - nickel foil subjected to the electrochemical reaction at -500 mV (versus Ni/NiO electrode) in 5M KOH solution. Reaction time (A) 2, (B) 4, (C) 6 and (D) 24 hours respectively.

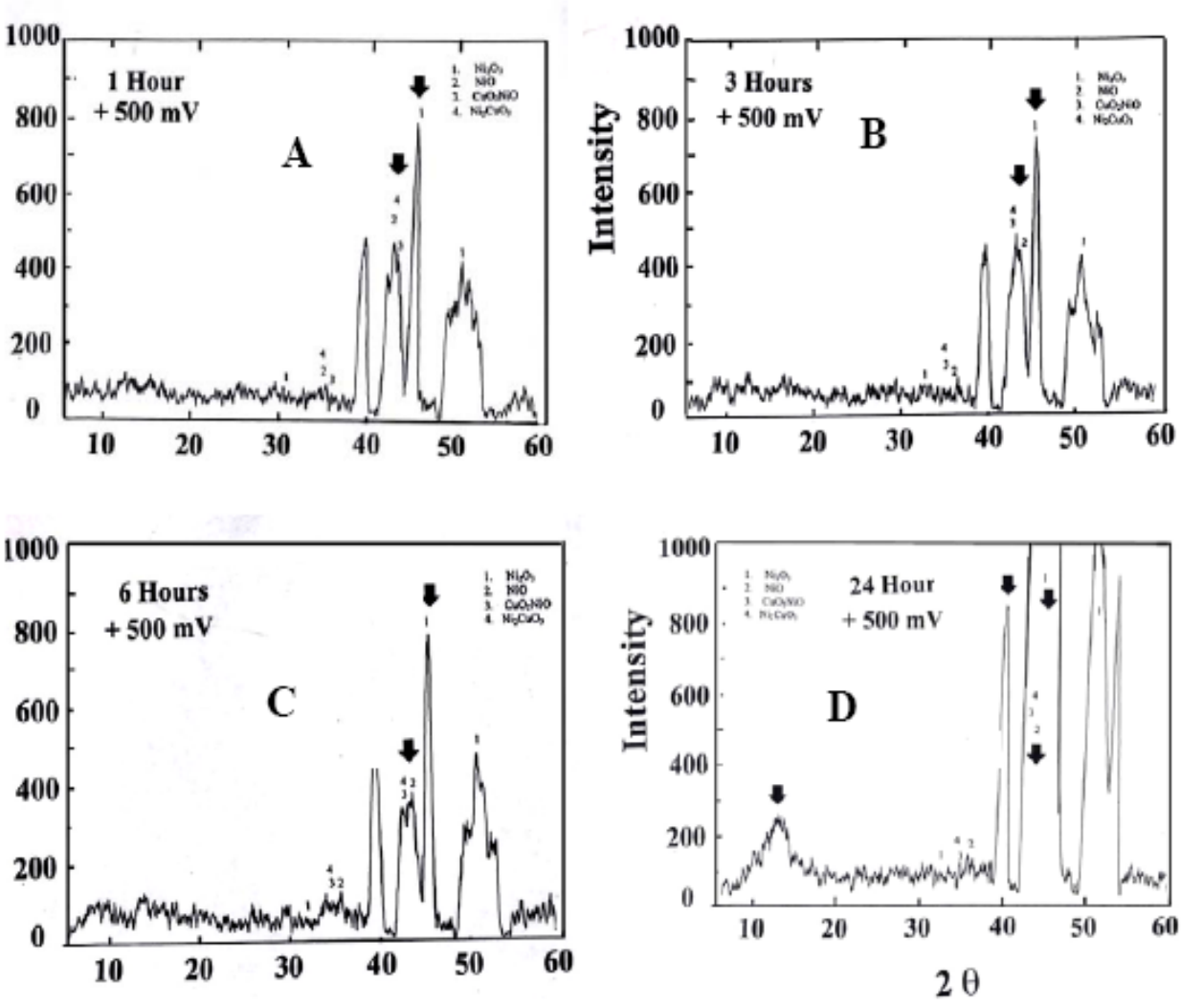

Figure 18. x-ray diffraction patterns obtained from 90-10 copper - nickel foil subjected to the electrochemical reaction at +500 mV (versus Ni/NiO electrode in 5 M KOH solution. Reaction time (A) 1, (B) 3, (C) 6 and (D) 24 hours respectively.

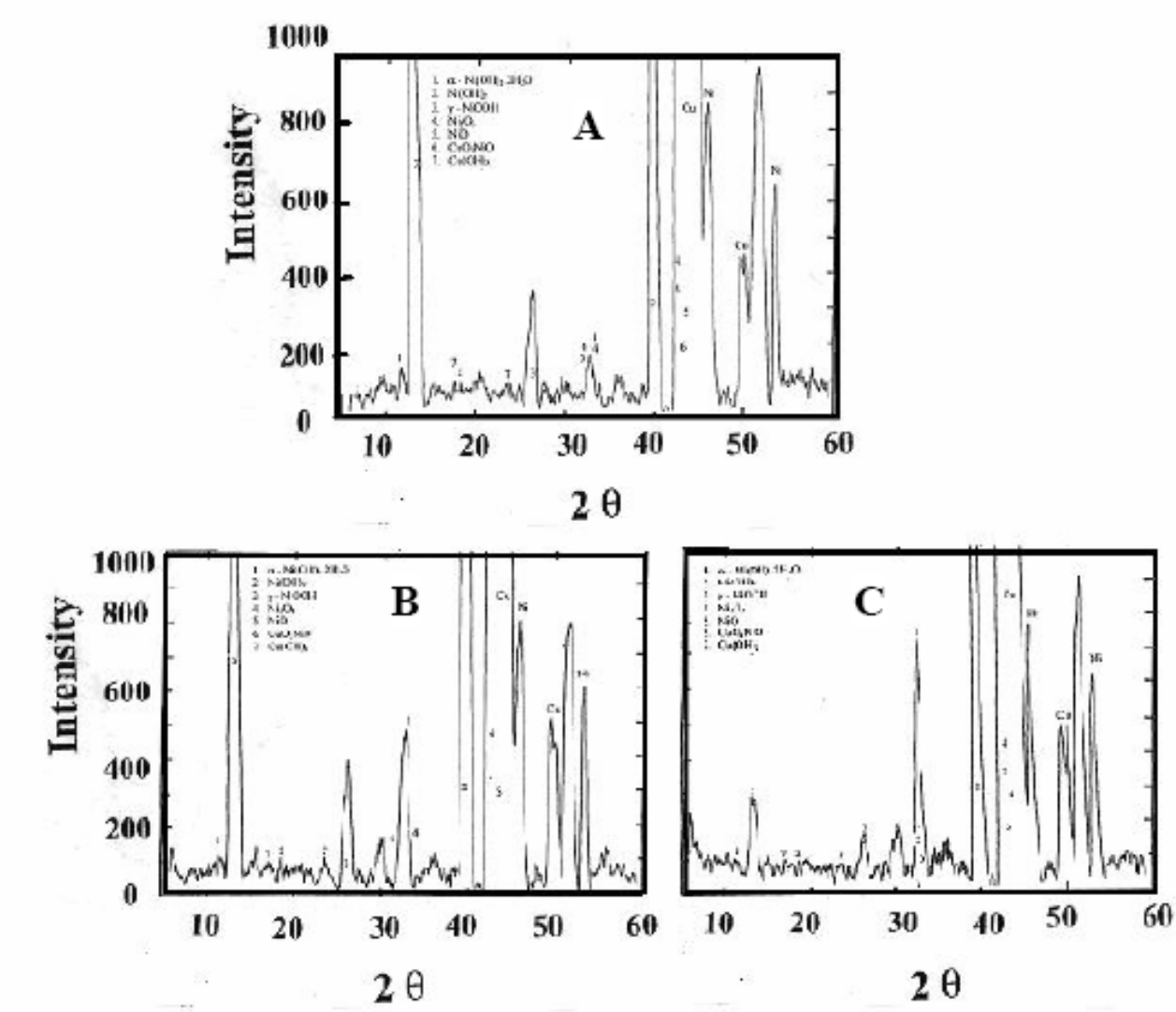

Figure 19. x-ray diffraction patterns obtained from 70-30 copper - nickel foil subjected to the electrochemical reaction at -100 mV (versus Ni/NiO electrode) in 5 M KOH solution. Reaction time (A) 2, (B) 4, and (C) 24 hours respectively.

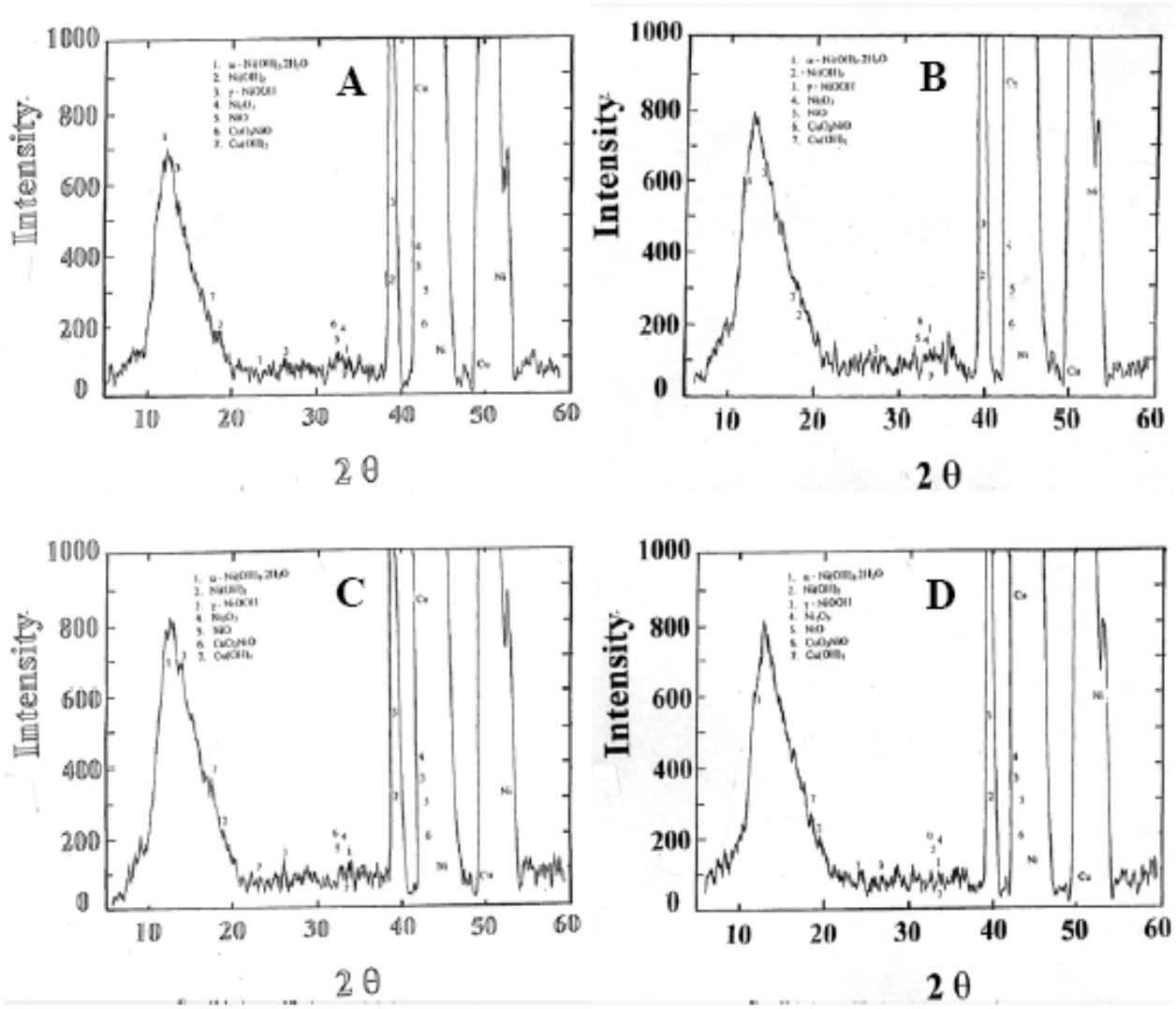

Figure 20. x-ray diffraction patterns obtained from 70-30 copper - nickel foil subjected to the electrochemical reaction at +100 mV (versus Ni/NiO electrode) in 5 M KOH solution. Reaction time (A) 2 , (B) 4, (C) 6 and (D) 24 hours respectively.

Figures 17 through 20 represent the x-ray diffraction data obtained from copper - nickel alloy during the electrochemical reaction progress for copper nickel samples in KOH or seawater. The results shown in the Figures 13 through 17 suggest that the peaks for metal in KOH are distinct and the peaks are very sharp and well defined. For metal/seawater system, the intensities were not well defined and the peaks are often not sharp. However, from careful examination of the results obtained in metal/KOH interface, the metal - seawater results were analyzed.

It is known from electrochemistry that during cathodic reaction, a reduction takes place and during anodic reaction, oxidation occurs. For example, during the cathodic reaction (-mV), of nickel, the γ-NiOOH that was present on the foils surface was reduced to $Ni(OH)_2$. Similarly, during the anodic reaction (+mV), the $Ni(OH)_2$ present on the surface will be oxidized to NiO and or Ni_2O_3 respectively [2-4]. The results shown in Figures 13 - 16 also support such a behavior. In order to quantify the ratio between the reactants and products the XRD data was reanalyzed. The area under a specific curve of γ-NiOOH and the $Ni(OH)_2$ was measured. Assuming that at the beginning of the electrochemical reaction (i.e. t = 0), the amount of γ-NiOOH is ≈ 100% while the amount of $Ni(OH)_2$ present is zero percent. As the reaction proceeds, the conversion of γ-NiOOH into $Ni(OH)_2$ continues and at time 't', the amount of γ-NiOOH reduced is equal to the amount of $Ni(OH)_2$ formed. The area under both γ-NiOOH and $Ni(OH)_2$ also change. The percent conversion can thus be equated to the duration of the chemical reaction.

Figures 13 and 14 show typical plots obtained from nickel in KOH both at - 800mV (versus Ni/NiO electrode) and +450 mV (versus Ni/NiO electrode). A schematic diagram illustrating the estimation for the normalized oxide conversion corresponding to the reaction at time 't' is given in Figure 21. From such plots, the normalized oxide was determined as a function of reaction time. The data was plotted and a best possible curve was hand drawn. From the lowest and highest value noted for reaction at a specific time, the error was determined. Two more reaction kinetics curves were generated using the positive and negative error to the normalized oxide growth versus the reaction time data. Figures 22 - 33 show typical plots of the normalized oxide growth versus the reaction time for Ni in KOH, and in seawater; 90-10 or 70 - 30 Cu - Ni in KOH and sea water respectively. The normalized plots consist of three different curves. The curves represent an *upper and lower limit of the data points* while the third curve represents an average value. The curve representing the average value was used to determine the values of the rate constants and the order of the electrochemical reaction. The rate of the reaction (i.e. the oxide growth) and the order of reaction that was determined for nickel in seawater, and 90-10 and 70-30 copper - nickel alloy in KOH and seawater are given in Tables 4 and 5 respectively.

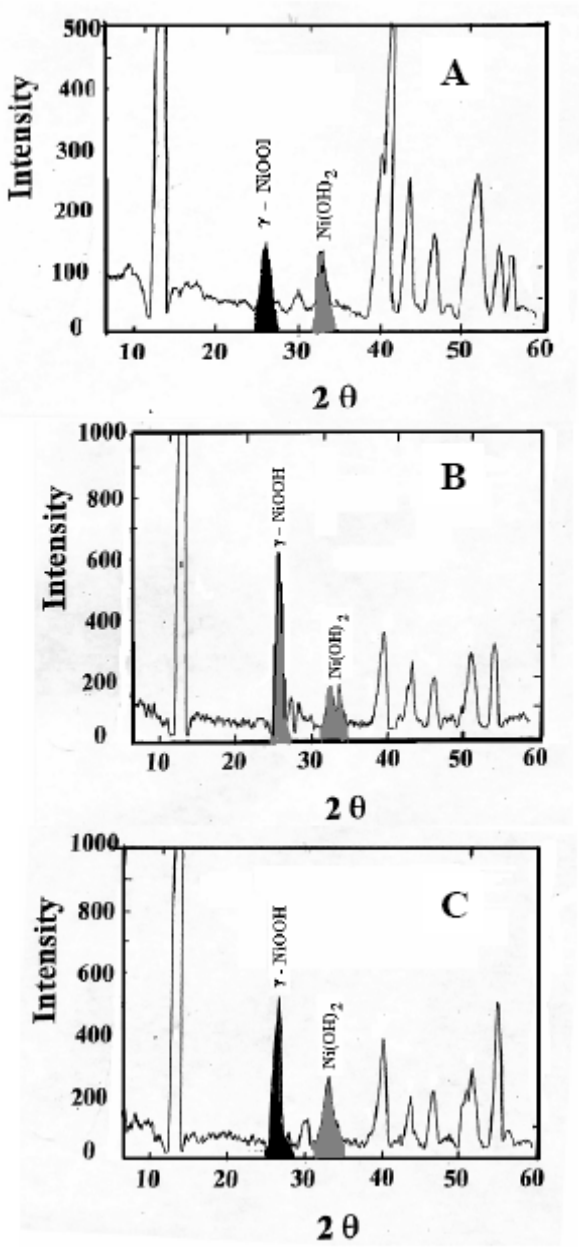

Figure 21. Schematic diagram showing how the normalized $Ni(OH)_2$ formed due to cathodic reaction. (A) after 2 hours, (B) after 4 hours and (C) after 24 hours of reaction time.*

* At 't' = 0; γ - NiOOH on the surface ≈ 100% and $Ni(OH)_2 \approx 0$.
At any time amount of $Ni(OH)_2$ formed ≈
Area under $Ni(OH)_2$ peak / Area under γ - NiOOH peak + Area under $Ni(OH)_2$ peak

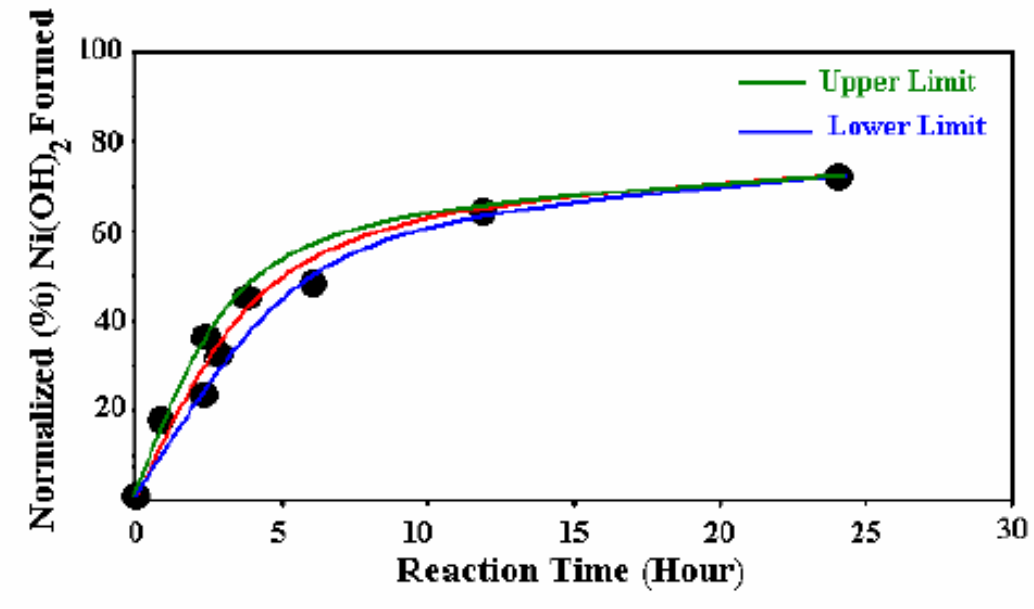

Figure 22. Normalized (%) $Ni(OH)_2$ formed during cathodic reaction for nickel in KOH solution. The applied potential was -800 mV (versus Ni/NiO electrode).

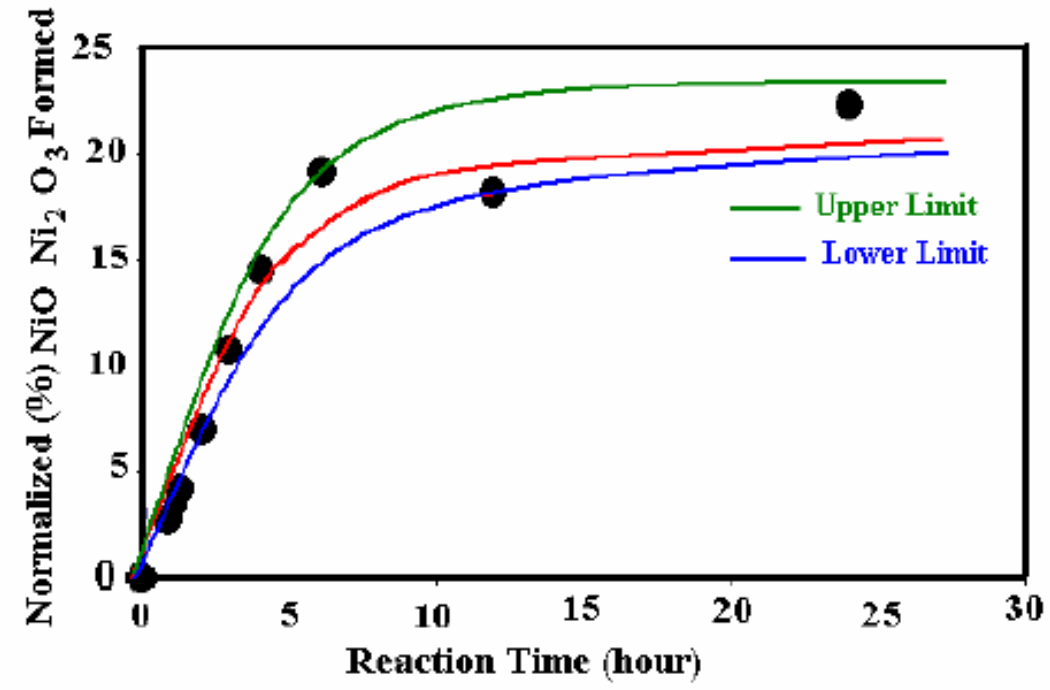

Figure 23. Normalized (%) NiO and Ni_2O_3 formed during anodic reaction for nickel in KOH solution. The applied potential was +450 mV (versus Ni/NiO electrode).

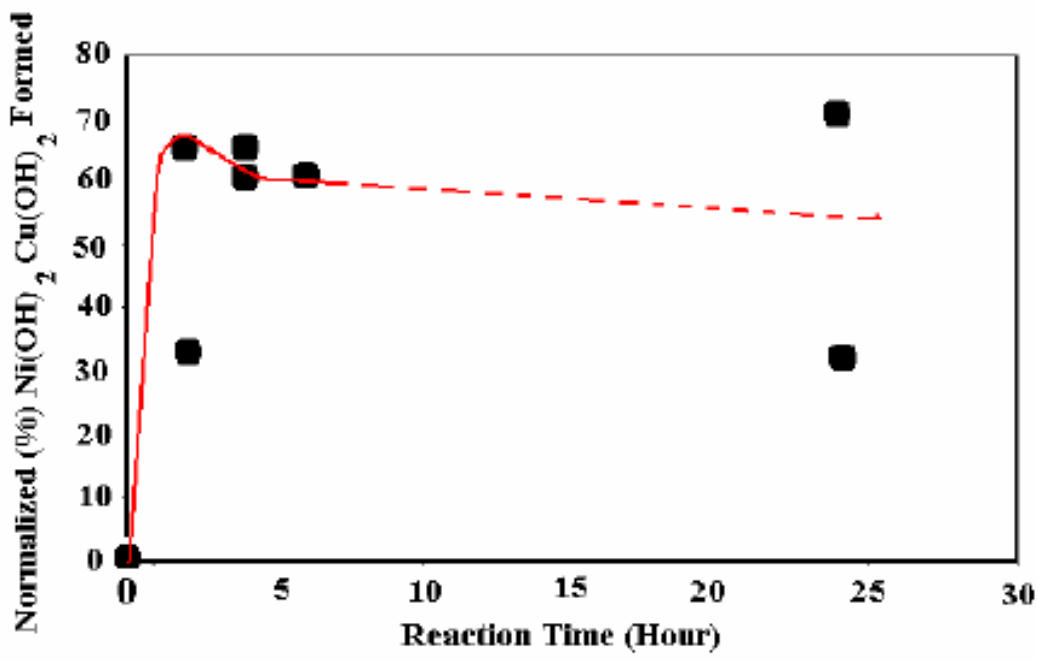

Figure 24. Normalized (%) Cu_2O, Cu_2O.NiO, NiO and Ni_2O_3 formed during cathodic reaction for 90-10 Cu-Ni alloy in KOH solution. The applied potential was -500 or -100 mV (versus Ni/NiO electrode).

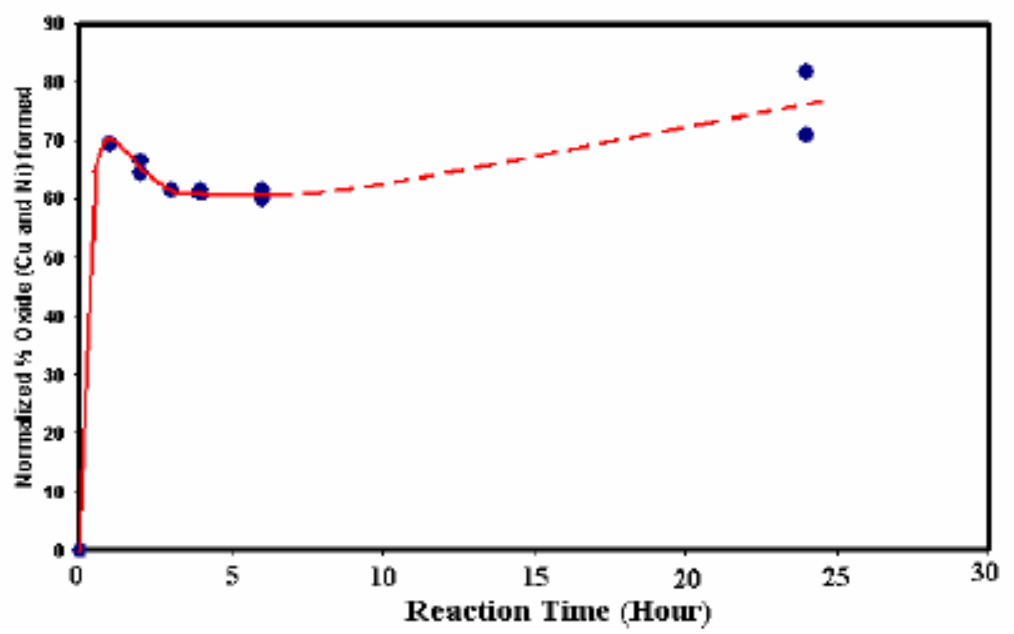

Figure 25. Normalized (%) Cu_2O, Cu_2O.NiO, NiO and Ni_2O_3 formed during anodic reaction for 90-10 Cu-Ni alloy in KOH solution. The applied potential was +500 or +100 mV (versus Ni/NiO electrode).

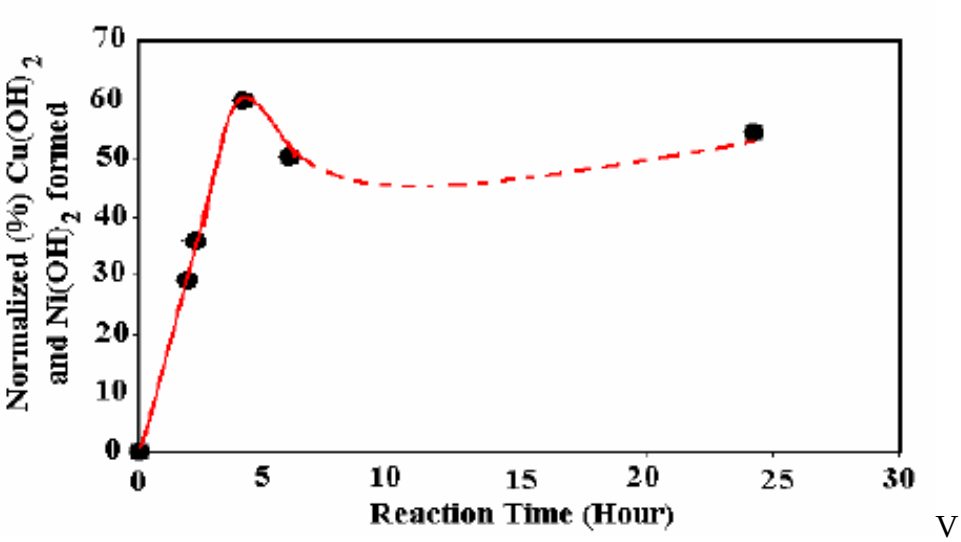

V

Figure 26. Normalized (%) $Cu(OH)_2$, $Ni(OH)_2$ formed during cathodic reaction for 70-30 Cu-Ni alloy in KOH solution. The applied potential was either -500 or -100 mV (versus Ni/NiO electrode).

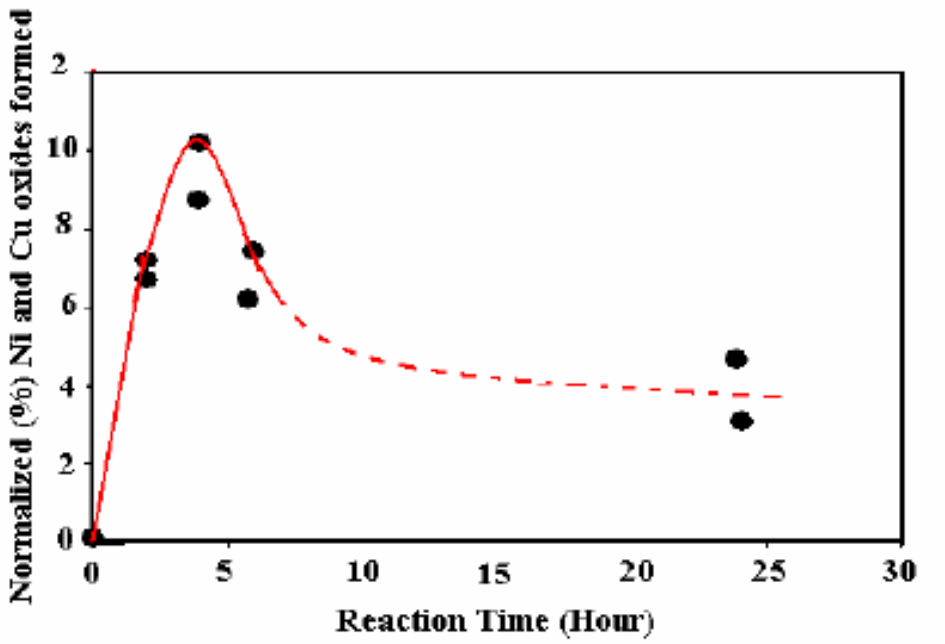

Figure 27Figure 27. Normalized (%) Cu_2O, $Cu_2O.NiO$, NiO and Ni_2O_3 formed during anodic reaction for 70-30 Cu-Ni alloy in KOH solution. The applied potential was either +500 or +100 mV (versus Ni/NiO electrode).

Table 4. Rate of reaction and the order of reaction for the electrochemical process at the nickel / 5M KOH solution.

System	Reaction in KOH		Over all Reaction		Stage I		Stage II	
	Cathodic Reaction (- mV)	Anodic Reaction (+ mV)	Rate (k) % /hour	Order (n)	Rate (k_1) % / hour	Order (n_1)	Rate (k_2) %/hour	Order (n_2)
Ni	- 800 mV γ - NiOOH → α - $Ni(OH)_2.2H_2O$		10.5	0.5	13.3	1.0	0.83	0
		+ 450 mV $Ni(OH)_2$ → Ni_2O_3 & NiO	2.9	0.5	3.57	1.0	0.79	0

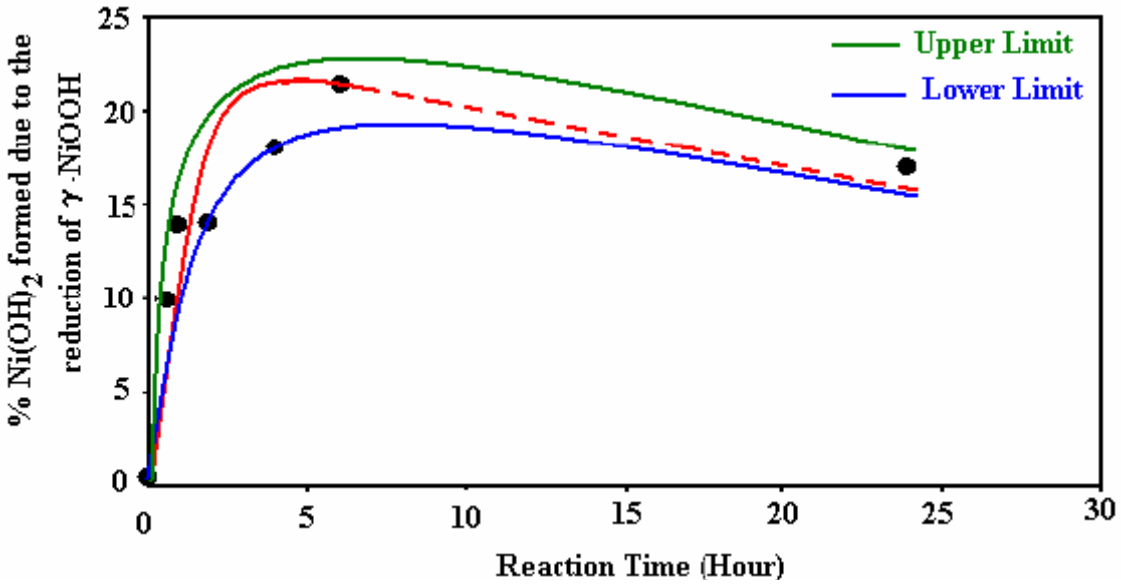

Figure 28. Normalized (%) $Ni(OH)_2$ formed during cathodic reaction for nickel foil in seawater solution. The applied potential was -800 mV (versus Ni/NiO electrode).

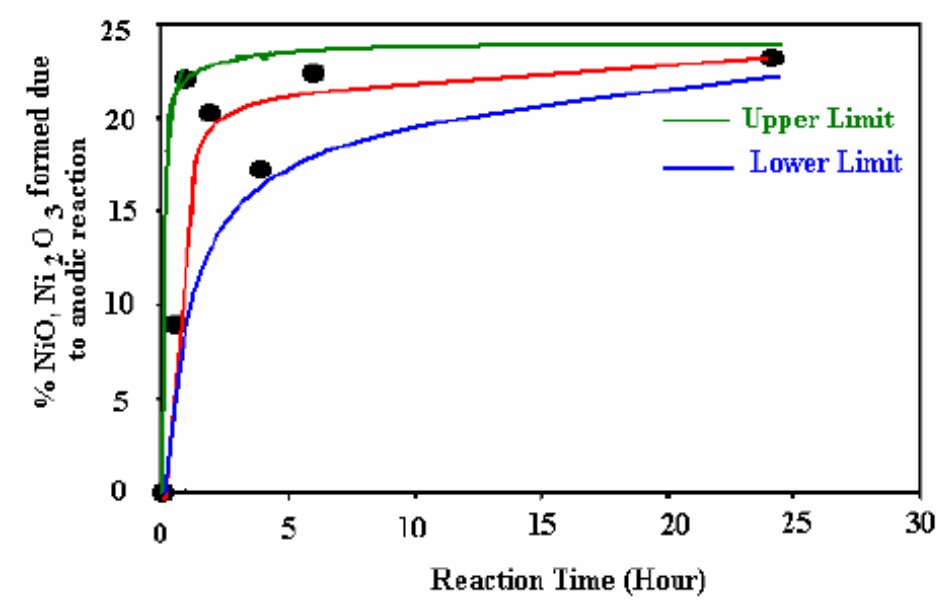

Figure 29. Normalized (%)NiO and Ni_2O_3 formed during anodic reaction for nickel foil in seawater solution. The applied potential was +450 mV (versus Ni/NiO electrode).

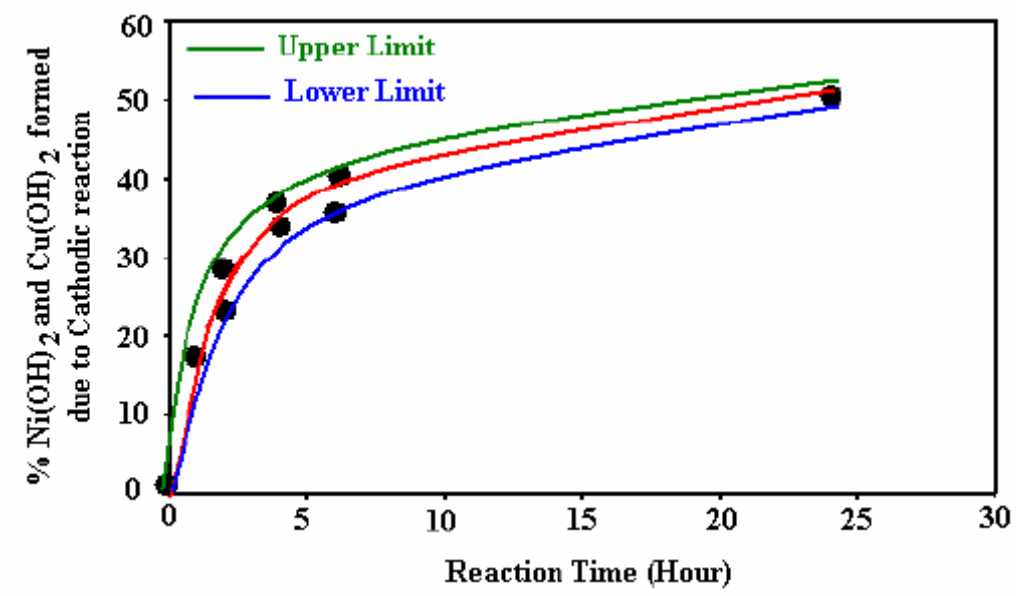

Figure 30. Normalized (%) $Cu(OH)_2$, $Ni(OH)_2$ formed during cathodic reaction for 90-10 Cu-Ni alloy in seawater solution. The applied potential was either -500 or -100 mV (versus Ni/NiO electrode).

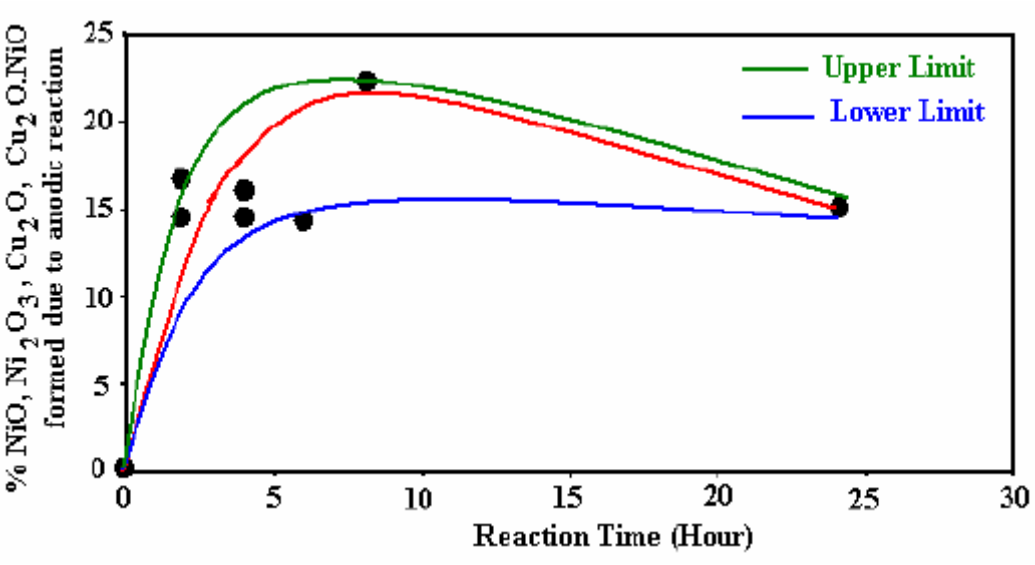

Figure 31. Normalized (%) Cu_2O, $Cu_2O.NiO$, NiO and Ni_2O_3 formed during anodic reaction for 90-10 Cu-Ni alloy in seawater solution. The applied potential was either +500 or +100 mV (versus Ni/NiO electrode).

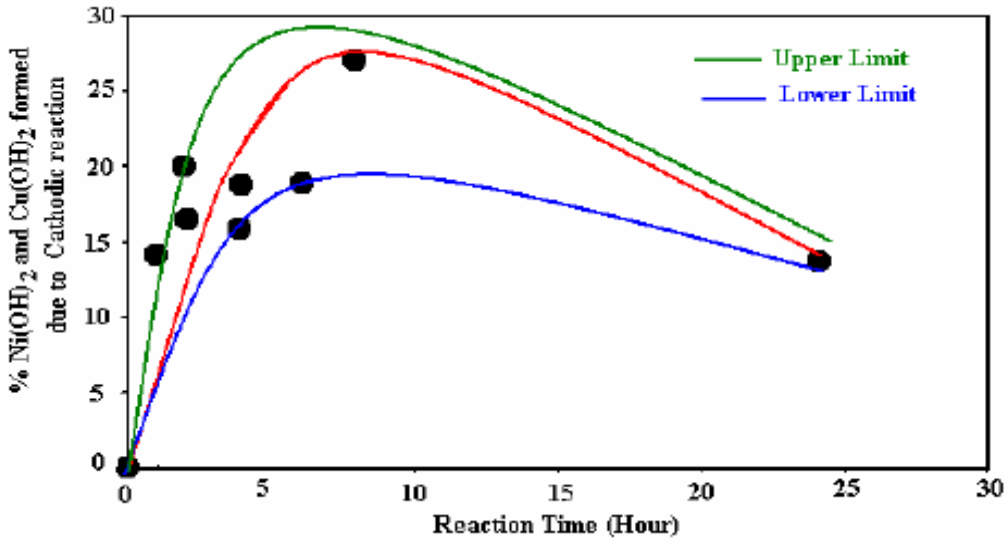

Figure 32. Normalized (%) $Cu(OH)_2$, $Ni(OH)_2$ formed during cathodic reaction for 70-30 Cu-Ni alloy in seawater solution. The applied potential was either -500 or -100 mV (versus Ni/NiO electrode).

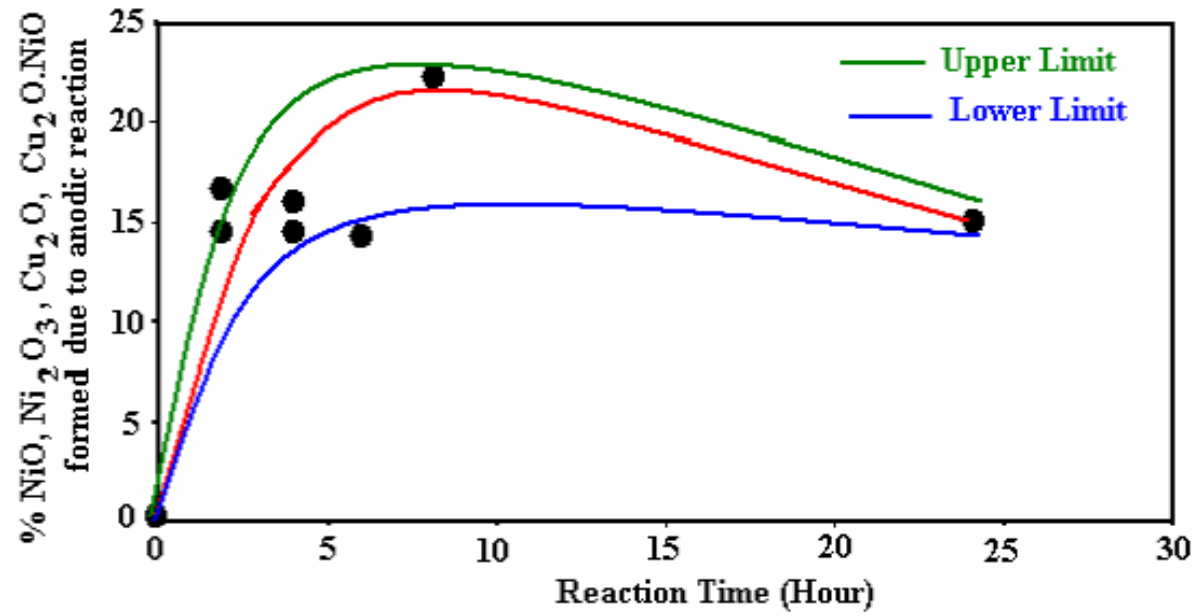

Figure 33. Normalized (%) Cu_2O, Cu_2O.NiO, NiO and Ni_2O_3 formed during anodic reaction for 70-30 Cu-Ni alloy in seawater solution. The applied potential was either +500 or +100 mV (versus Ni/NiO electrode).

Table 5. Rate of reaction and the order of reaction for the electrochemical process at the nickel - sea water solution.

System	Overall Reaction		Stage I		Stage II		Stage III	
	Rate (k) [%/hour]	Order (n)	Rate (k) [%/hour]	Order (n)	Rate (k) [%/hour]	Order (n)	Rate (k) [%/hour]	Order (n)
Cathodic Reaction (-800 mV)	8	0.5	12.5	1.5	1.95	0.5	0.4	0
Anodic Reaction (+450 mV)	12	0.5	15	1.0	5	0	0.53	1.0

Table 6. Rate of the reaction and the order of the reaction for the electrochemical process at the 90-10 and 70-30 copper nickel alloy seawater interface.

System	Reaction in Seawater	Overall Reaction		Stage I		Stage II		Stage III	
		Rate (k) [%/hour]	Order (n)	Rate (k) [%/hour]	Order (n)	Rate (k) [%/hour]	Order (n)	Rate (k) [%/hour]	Order (n)
90-10 Cu-Ni	Cathodic Reaction (- mV)	12	0.5	15	1.0	5	0	0.53	1.0
	Anodic Reaction (+ mV)	6.67	1.0	10	1.0	2.05	0	0.13	0.5
70 –30 Cu-Ni	Cu-Ni Cathodic Reaction (- mV)	6.67	0.5	15	1.0	2.39	0	-0.6	0.5
	Anodic Reaction (+ mV)	3.35	-	6.25	-	-	-	-	-

The electrochemical reaction kinetic parameters (viz. the reaction rate and order of reaction) determined from the x-ray diffraction data on nickel in KOH or seawater suggest that the reaction kinetics is smooth and the rate process is controlled by the diffusion of liquid through the oxide layer. The order of reaction during the fast oxide buildup is one, indicating that the metal is the only active participant (whose concentration changes with time) in the reaction. The slow oxide buildup is a time dependent process. Further, the results also suggest that the oxide formation process can be treated as a process in which the oxide layer buildup is uniform.

The results of copper nickel alloys (90-10 and 70-30) in KOH suggest that the oxide buildup is not uniform and the difference is perhaps due to the difference in the rate of the oxide formation of copper and nickel in solution.

From the structural analysis data, it is clear that the oxide formation in copper–nickel alloys is not a homogeneous process. The observed scatter in the present potential data on the nickel aluminum bronze in ammonia solution and seawater can therefore be attributed to the difference in the rate of oxidation of the metallic components of the alloy.

By comparing the information obtained based on the structural analysis performed on nickel and copper - nickel in KOH and seawater and the potential measurements on nickel aluminum bronze in ammonia and seawater, the oxide formation on nickel aluminum bronze alloy can be suggested schematically as follows. Consider a sample of NAB is in contact with seawater or ammonia solution and at the start of the reaction (t = 0), only the air oxide is present and no corrosion products were formed on the sample surface (Figure 34 (A)). As the exposure time is increased, different metallic species form their oxides and deposit on the metal surface. The deposition is uneven and the surface is heterogeneous (Figure 34(B)). The surface potential will vary and tend to change significantly. As the reaction is continued, some of the deposited oxide may dislodge and fall of from the oxide layer, or re-dissolve into solution. Eventually the whole surface will be covered with an oxide layer (Figure 34(C) and (D)). The potential at this time will have a specified value. Furthermore, continued exposure of the oxide-coated alloy to the solution will exhibit a complex electrochemical process. That is, the rate of the depletion of different metallic species of the alloy will be different. This is because while one metal (viz. aluminum) may form a passive oxide layer, the other (viz. copper) may continue to deplete at much faster rate. Such a process will lead to higher copper based hydroxide and oxy-hydrate formation than that of aluminum hydroxide formation. The result is that the measured surface oxide potential will correspond to more of copper based hydroxide than the aluminum based oxides. Such a selective metal dissolution process of the alloy will increase the scatter in the measured potentials. However, prolonged electrochemical reaction will establish a steady state condition and the scatter in the measured potentials will decrease. The final result will be a smooth measured potential versus reaction time plot that shows a clear and a systematic kinetics based chemical reaction trend.

Although the above conclusions appear to explain the observed anomalies, the present report is based on two separate investigations that were carried out for different reaction times. For example, the structure of nickel and copper–nickel alloys in KOH and seawater was

determined for experiments carried out for 24 hours only. The potential measurements presented in Table 1a and 1b were made for up to 34 days. The potentials represent a cumulative value of the alloy surface and it does not represent any one single oxide. The value is averaged over the sample surface area.

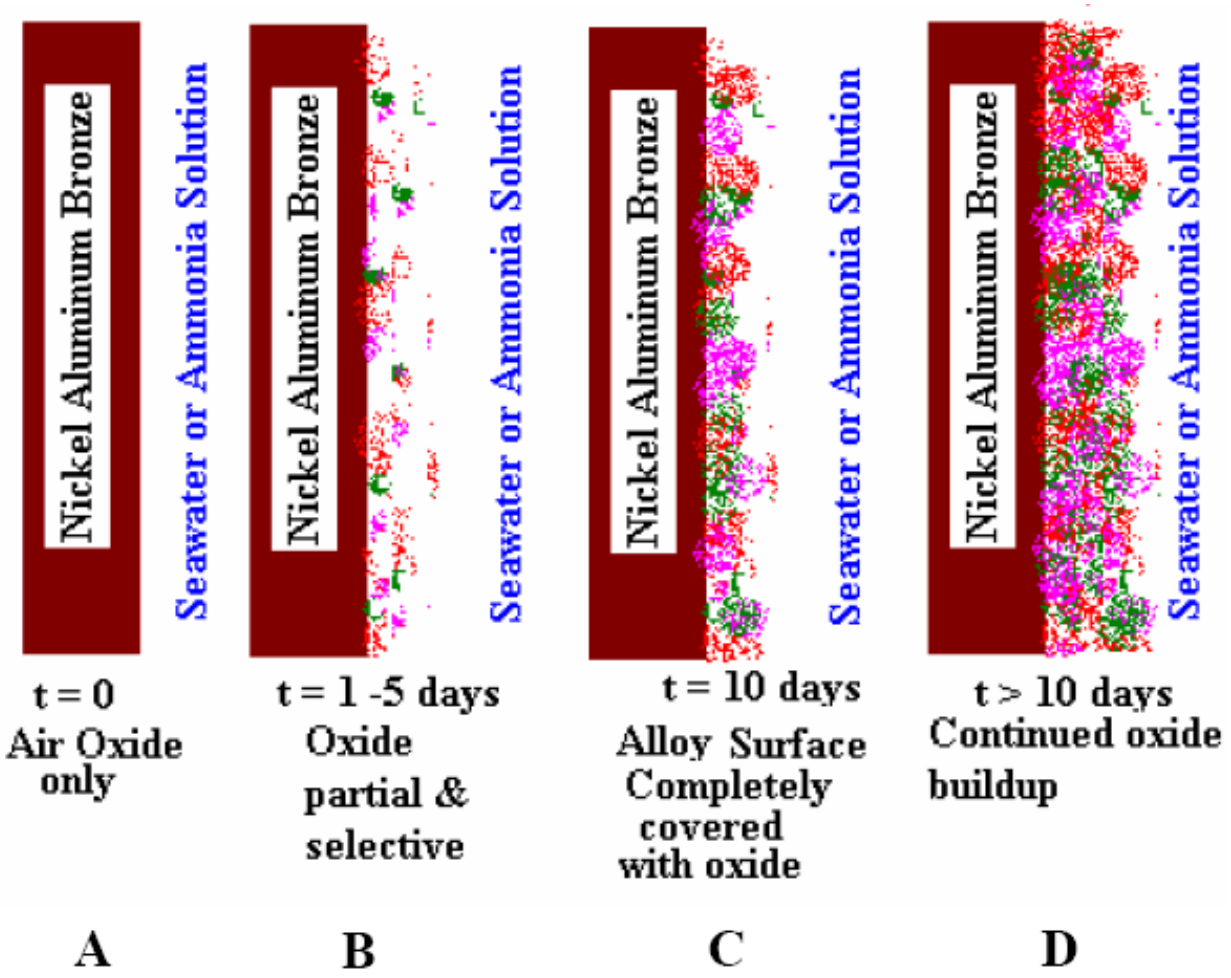

Figure 34. Schematic diagram of oxide growth on nickel aluminum bronze in seawater and or ammonia solution. Different colors represent different oxides such as copper oxide, nickel oxide and aluminum oxide.

It will be interesting to see whether better information on the structure of different oxides can be obtained from oxidized sample surfaces exposed for longer periods. If such information can be generated from a systematic study, it will not only provide electrochemical kinetic parameter data, but also validates and establishes a new methodology to determine corrosion characteristics of alloys and the selective corrosion behavior of the each metallic species, based the electrical potential measurement.

Conclusion

The following conclusions can be made from the present analysis:

The kinetic parameters of the electrochemical/corrosion process of nickel aluminum bronze (NAB) samples in different corrosion liquid media can be determined from the electrical potential measurements.

1. The present analysis indicates that the corrosion behavior of NAB in seawater is completely different to that of the corrosion behavior in ammonia – water mixtures.

2. The rate of corrosion of NAB in 10%-90% and 20%-80% ammonia - water is slower than the corrosion in 50%-50% ammonia – water mixture. Therefore the oxide build up in 10 and 20% ammonia will be uniform and the packing will be much more dense than the oxide buildup due to corrosion in 50% ammonia. The overall electrochemical rate in the former case (NAB-10%-90% and NAB-20% - 80% ammonia - water systems) is determined by the diffusion process, while in NAB-50%-50% ammonia water system, the overall rate depends upon the change in concentration of metal surface and the diffusion process.

3. The electrochemical process in all samples investigated here is dominated by selective corrosion. Therefore, the surface oxide composition is not uniform. The consequence is that during the first 10 days of electrochemical reaction, the measured potential data shows large scatter.

4. Continued exposure of the NAB sample to the corroding liquid beyond 10 days, reduces the scatter.

5. The in-situ studies on nickel and (90%-10% and 70%-30%) copper - nickel alloys in KOH and seawater also suggested that some of the samples exhibit considerable scatter in the reaction kinetics data.

6. The x-ray structural analysis revealed preferential or selective oxidation of nickel as nickel hydroxides than the copper as copper oxide.

References

1. Wong, C. and K. L. Vasanth, “Initiation of Stress Corrosion Cracking Initiation in Nickel Aluminum Bronze”, ONR FY 2004 End of Year Report.

2. Srinivasa Rao, A., “Characterization of Surface Film Growth During Corrosion Process”, EPRI Technical Report # 1000863, Oct. 2000.

3. Srinivasa Rao, A., *Characterization of Surface Film Growth During Electrochemical Process: Nickel / Nickel Alloys in Sea Water*, Naval Surface Warfare Center, West Bethesda MD, Technical Report, NSWCCD-61-TR-02/15, Aug 2002.

4. Srinivasa Rao, A. and J. N. Murray, *Evaluation of Hydroxyethane Diphosphonic Acid (HEDPA) as Metal Cleaning Agent Using Chemical and Electrochemical Test Methods: Part – 1*, Naval Surface Warfare Center, West Bethesda MD, Technical Report CARDIVNSWC-TR-61-98-16, Jun 1998.

Distribution

copies

DOD - CONUS

CHIEF OF NAVAL RESEARCH
ATTN CODE 332 CORROSION PROGRAM MANAGER(AIRAN J. PEREZ) 1
875 N. RANDOLPH STREET
ARLINGTON VA 22203-1995

COMMANDER
NAVAL SEA SYSTEM COMMAND
ATTN SEA 05M (KAZNOFF) 1
1333 ISAAC HULL AVE SE STOP 5130
WASHINGTON NAVY YARD DC 20376-5130

COMMANDER
NAVAL SEA SYSTEMS COMMAND
ATTN SEA 05M2 1
1333 ISAAC HULL AVE SE STOP 5132
WASHINGTON NAVY YARD DC 20376-5132

COMMANDER
NAVAL SEA SYSTEMS COMMAND
ATTN SEA 05M1 1
1333 ISAAC HULL AVE SE STOP 5132
WASHINGTON NAVY YARD DC 20376-5132

INTERNAL

CODE 0115		1
CODE 0112		1
CODE 60		1
CODE 60	(SUDDUTH)	1
CODE 60	(RULE)	1
CODE 61		1
CODE 612	(RAO)	6
CODE 611		1
CODE 612		1
CODE 612	(CZYRYCA)	1
CODE 612	(FIELDER)	1
CODE 612	(GAIES)	1
CODE 612	(HAYDEN)	1
CODE 612	(PURTSCHER)	1
CODE 612	(ROE)	1
CODE 612	(STILES)	1
CODE 612	(SUTTON)	1
CODE 612	(SYLVESTER)	1
CODE 612	(WONG)	1
CODE 612	(ZHANG)	1
CODE 612	(BRANDEMARTE)	1
CODE 613		1
CODE 614		2
CODE 615		1
CODE 616		1
CODE 617		1
CODE 62		1
CODE 63		1
CODE 64		1
CODE 65		1
CODE 66		1
CODE 3442	(TIC – pdf only)	

This page intentionally left blank

Carderock Division